

Spectral stability and perturbation results for kernel differentiation matrices on the sphere

T. Hangelbroek*, C. Rieger†, G. Wright‡

Abstract

We investigate the spectrum of differentiation matrices for certain operators on the sphere that are generated from collocation at a set of “scattered” points X with positive definite and conditionally positive definite kernels. We focus on cases where these matrices are constructed from collocation using all the points in X and from local subsets of points (or stencils) in X . The former case are called global methods (e.g., the Kansa or radial basis function (RBF) pseudospectral method), while the latter are referred to as local methods (e.g., the RBF finite difference (RBF-FD) method). Both techniques are used extensively for numerically solving certain partial differential equations on spheres, as well other domains. For time-dependent PDEs like the diffusion equation, the spectrum of the differentiation matrices and their stability under perturbations are central to understanding the temporal stability of the underlying numerical schemes.

In the global case, we present a perturbation estimate for differentiation matrices which discretize operators that commute with the Laplace-Beltrami operator. In doing so, we demonstrate that if such an operator has negative spectrum, then the differentiation matrix does, too. For conditionally positive definite kernels this is particularly challenging since the differentiation matrices are not necessarily diagonalizable. This perturbation theory is then used to obtain bounds on the spectra of the differentiation matrices that arise from a local method using conditionally positive definite surface spline kernels. Numerical results are presented to confirm the theoretical estimates.

Keywords: Kansa method, RBF Pseudospectral, Hurwitz stability, local Lagrange, RBF-FD

MSC Codes: 65D12, 65D25, 65M06, 65M20, 65N12

1 Introduction

Kernel-based collocation methods have become increasingly popular for approximating solutions of partial differential equations (PDEs) on spheres, \mathbb{S}^d , and other smooth surfaces as they do not require a grid or mesh and they can produce high-orders of accuracy (e.g., [13, 14, 19, 20, 29, 38, 44]). These methods are typically formulated in terms of differentiation matrices (DMs) that approximate the underlying continuous spatial differential operators, generically denoted by \mathcal{L} , of the PDE at a set of “scattered” nodes (or point cloud) X . For time-dependent problems, these kernel-based collocation methods are typically used in a method-of-lines approach, where the spatial derivatives are approximated by DMs and some initial value problem solver is used to advance the semi-discrete system in time [16].

The success of this technique in terms of temporal stability is fundamentally dependent on properties of the spectrum of the DMs. For example, from classical linear stability analysis, a necessary condition for the method-of-lines scheme to be stable in time is that

*Department of Mathematics, University of Hawai‘i – Mānoa, 2565 McCarthy Mall, Honolulu, HI 96822, USA, hangelbr@math.hawaii.edu. Research supported by by grant DMS-2010051 from the National Science Foundation.

†Philipps-Universität Marburg, Department of Mathematics and Computer Science, Hans-Meerwein-Straße 6, 35032 Marburg, Germany, riegerc@mathematik.uni-marburg.de

‡Boise State University, 1910 University Drive, 83725, Boise, Idaho, USA, gradywright@boisestate.edu. Research supported by by grants DMS-1952674 and DMS-2309712 from the National Science Foundation.

the spectrum of the DM associated with the spatial derivatives of the PDE (scaled by the time-step) is contained in the stability domain of the initial value problem solver. At the very least, this condition generally requires that the real part of the eigenvalues of the DM are negative, or non-positive (i.e., the DM is Hurwitz stable). While there are several numerical studies that investigate the spectral properties of kernel-based DMs on spheres and more general surfaces (e.g., [13, 15, 19, 29]), there are surprisingly very few theoretical results in the literature despite the increasing popularity of these methods. One reason for this may be that the kernel-based DMs do not immediately inherit any symmetry properties of \mathcal{L} (e.g., self-adjointness). The aim of this article is to partially fill this gap by developing a spectral stability theory (and an associated perturbation theory) of DMs that arise from discretizations of operators that commute with the Laplace-Beltrami operator Δ . This has application to a wide class of semi-linear parabolic PDEs on spheres, including reaction diffusion equations for modeling pattern formation and chemical signaling [19].

It is worth noting that there are some existing theoretical results on temporal stability of the semi-discrete systems. For example, the study [35] shows that DMs for certain operators \mathcal{L} on \mathbb{S}^2 have real spectra (a property sometimes called aperiodicity), although this is not sufficient to guarantee Hurwitz stability. Another study [20] demonstrates “energy stability” for a global collocation method of the heat equation on \mathbb{S}^2 based on positive definite kernels (this is also a consequence of our results, addressed in Section 5.1, and generalized to the conditionally positive definite case). Finally, some recent works have theoretically studied temporal stability of kernel collocation methods on planar domains using a different approach [21, 41]. These studies have primarily focused on hyperbolic PDEs and employ oversampling (or least squares formulations) to demonstrate “energy stability”.

1.1 Differentiation matrices

The global (or Kansa or pseudospectral) kernel-based collocation approach of constructing a DM associated with a given set of distinct points $X \subset \mathbb{S}^d$ for the differential operator \mathcal{L} is based on interpolation with a positive definite (PD) or conditionally positive definite (CPD) kernel $\Phi : \mathbb{S}^d \times \mathbb{S}^d \rightarrow \mathbb{R}$ using all points in X . Such DMs can be defined naturally using the Lagrange basis $\{\chi_j\}_{x_j \in X}$ for the trial space $\text{span}_{x_\ell \in X} \Phi(\cdot, x_\ell)$ as

$$\mathbf{M}_X = \left(\mathcal{L}\chi_j(x_k) \right)_{j,k}. \quad (1)$$

Note that the precise definition of a PD or CPD kernel is given in section 2, and the construction of this DM is described in more detail in section 3.

While DMs based on this global method can be computationally expensive to compute since they use all the points in X , they have theoretical appeal, at least for certain elliptic problems. For example, in [12], it is shown that, for PD kernels and operators like $\mathcal{L} = 1 - \Delta$, \mathbf{M}_X is invertible with a modest stability bound, see [12, Proposition 4.4], and that the spectrum of \mathbf{M}_X is strictly positive. One of the primary motivations of this paper is to show that similar results hold for CPD kernels and more general operators \mathcal{L} involving polynomials of Δ . For example, for the simpler case of $\mathcal{L} = -\Delta$, we prove that the spectrum of \mathbf{M}_X is real and non-negative, as illustrated for a particular $X \subset \mathbb{S}^2$ in Figure 1 (\times markers).

A more computationally efficient approach considers instead constructing a DM by approximating \mathcal{L} using kernel-collocation over local subsets (or stencils) of X . One of these techniques uses a “local Lagrange functions”, $\{b_j\}$, generated by a PD or CPD kernel Φ , but only using a small stencil $\Upsilon_j \subset X$ consisting of points near to x_j , so that $b_j(x_k) = \delta_{j,k}$ for $x_k \in \Upsilon_j$. In this case the DM, which we denote by \mathbf{M}_X^{LL} , is sparse and is given by

$$\left(\mathbf{M}_X^{\text{LL}} \right)_{j,k} = \begin{cases} \mathcal{L}b_j(x_k), & x_j \text{ near to } x_k, \\ 0, & \text{otherwise.} \end{cases} \quad (2)$$

For certain point sets X and kernels Φ , $\mathcal{L}b_j$ is very close to $\mathcal{L}\chi_j$ even for relatively small stencils. This is a consequence of results in [17], which considers local Lagrange bases for

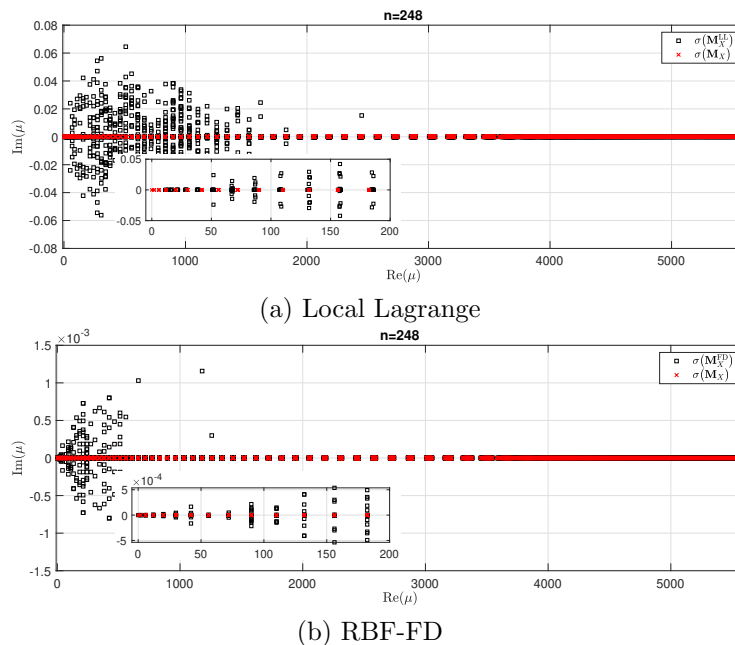


Figure 1: Comparison of the spectra of the DMs for the (negative) Laplace-Beltrami operator on \mathbb{S}^2 based on the global kernel collocation method (\mathbf{M}_X) and two local methods: (a) local Lagrange (\mathbf{M}_X^{LL}) and (b) RBF-FD (\mathbf{M}_X^{FD}). All results are for the CPD restricted surface spline kernel of order $m = 3$ and a minimum energy point set on \mathbb{S}^2 (described in section 2) with $N = 4096$ points. Both local DMs were computed using stencils with $n = 248$ points. Insets show the spectra near the origin of the complex plane.

certain CPD kernels on spheres (e.g., restricted surface splines), but has been generalized to other kernels on other manifolds [26]. Note that the local Lagrange approach is described in more detail in section 5.2. Another local technique is the radial basis function finite difference (RBF-FD) method, which has been used widely in many applications on surfaces and general Euclidean domains (e.g. [10, 14, 34, 38, 38, 40]). This method also constructs a sparse DM, which we denote by \mathbf{M}_X^{FD} , but it uses a different stencil-based kernel-collocation approach (as detailed in Section 5.3).

While these local methods are much more computationally efficient than the global method, it is more difficult to prove results about the spectral stability of their DMs because they do not have an underlying structure to exploit. Figure 1 shows that the spectra of DMs of both local methods are indeed more complicated than the global method. The approach we follow to study the spectral stability of the local DMs is to view them as perturbations of the the global DM, \mathbf{M}_X , and to bound their spectra in terms of the spectrum of \mathbf{M}_X . Indeed, both local methods recover \mathbf{M}_X in the limit that their stencils include every point in X . This motivates two problems:

- to determine the spectrum for the global DM \mathbf{M}_X when Φ is CPD
- to develop a perturbation theory for the spectrum of kernel-based DMs

Both of these problems are relevant beyond the specific motivation mentioned here. There are many reasons the DM might be perturbed (e.g. by small adjustments to the point set, or evaluation of the kernel, or by approximation of the differential operator, either from approximation or by addition of higher order “viscosity” terms), and it is common practice to supplement the kernel with an auxiliary polynomial space and provide corresponding constraints [14, Section 5.1] – in short, to treat a PD kernel as CPD.

Our spectral stability analysis is limited to the local Lagrange DMs \mathbf{M}_X^{LL} , where, for certain kernels and point sets X , recent results allow us to bound $\|\mathbf{M}_X^{\text{LL}} - \mathbf{M}_X\|$. Analogous results are not yet available for RBF-FD DMs, but we give numerical evidence that a similar stability analysis may hold.

1.2 Objectives and Outline

The main goals of this article are to produce a perturbation result for global kernel-based DMs on spheres for operators involving polynomials of Δ , and to employ this result to control the spectrum of nearby local Lagrange DMs. For strictly PD kernels, the first goal is achieved by using a fairly straightforward application of the Bauer-Fike theorem. However, the situation is considerably more challenging for CPD kernels, which produce DMs that are not obviously diagonalizable (and may have generalized eigenvectors). However, this is the apposite case for working with local Lagrange bases on spheres. A final objective is to show that the local Lagrange DMs constructed from the restricted surface spline kernels on \mathbb{S}^2 can have positive spectra.

The outline for the remaining sections of the paper are as follows. In section 2, we establish notation and give necessary background for spheres, including the spherical Laplace-Beltrami operator, the operators for which our theory applies, PD and CPD kernels on spheres, and point sets. Section 3 treats the perturbation of the global DMs generated by PD kernels. The perturbation result follows by estimating the conditioning of the eigenbasis for the DM and applying the Bauer-Fike theorem. This approach can be generalized to other settings (i.e., other choices of kernel/manifold/differential operator) and we discuss how this might be done at the end of section 3.

Section 4 introduces global DMs generated by CPD kernels. In section 4.1, we present Lemma 4.1, which shows that the DM for a CPD kernel is similar to a block-upper-triangular matrix with diagonal principal blocks. This factorization is sufficient to provide Proposition 4.3, which is a version of the Bauer-Fike theorem for DMs from CPD kernels. We then discuss necessary and sufficient conditions for the DM to be diagonalizable in section 4.3. Section 4.4 provides estimates of the (ℓ_2) matrix norms of various blocks appearing in the decomposition of Lemma 4.1 and which appear as terms in Proposition 4.3. Section 4.5 gives experimental evidence which suggests it is possible to improve the estimates of some of the matrix norms estimated in section 4.4, and therefore that the perturbation result Proposition 4.3 can be tightened.

Section 5 provides some applications of the theory from Sections 3 and 4 as well as some numerical results. Energy stability of certain semi-discrete problems is given in section 5.1. Section 5.2 applies the results of section 4 to the local Lagrange DMs \mathbf{M}_X^{LL} constructed from restricted surface spline kernels on \mathbb{S}^2 . In this setting, we show that it is possible to consider a relatively sparse \mathbf{M}_X^{LL} as a perturbation of the global DM \mathbf{M}_X that has a closely matching spectrum. In particular, if the spectrum $\sigma(\mathbf{M}_X)$ has strictly positive real part, then the spectrum of \mathbf{M}_X^{LL} will also have strictly positive real part for sufficiently large stencils or sufficiently dense point sets X . We illustrate these theoretical results on \mathbf{M}_X^{LL} with some numerical examples. Finally, we provide some numerical evidence that similar theoretical estimates may also hold for the RBF-FD DMs \mathbf{M}_X^{FD} .

2 Preliminaries

We denote the d -dimensional sphere as $\mathbb{S}^d = \{x \in \mathbb{R}^{d+1} \mid |x| = 1\}$ and let $\text{dist}(x_1, x_2) := \arccos(x_1 \cdot x_2)$ denote the Euclidean distance function for $x_1, x_2 \in \mathbb{S}^d$. The sphere has the usual spherical coordinate parameterization $(\theta_1, \dots, \theta_d) \mapsto (x_1, \dots, x_{d+1})$ by $\theta_1, \dots, \theta_d$

where $0 \leq \theta_j \leq \pi$ for $j = 1 \dots d-1$ and $0 \leq \theta_d \leq 2\pi$. Here

$$\begin{aligned} x_1 &= \cos \theta_1 \\ x_j &= \sin \theta_1 \cdot \sin \theta_2 \cdots \sin \theta_{j-1} \cdot \cos \theta_j \quad \text{for } j = 2 \dots d, \\ x_{d+1} &= \sin \theta_1 \cdot \sin \theta_2 \cdots \sin \theta_{d-1} \cdot \sin \theta_d. \end{aligned}$$

The Laplace-Beltrami operator on \mathbb{S}^d is a self-adjoint, negative semi-definite operator defined recursively as

$$\Delta_{\mathbb{S}^d} = \frac{1}{(\sin(\theta_1))^{d-1}} \frac{\partial}{\partial \theta_1} (\sin(\theta_1))^{d-1} \frac{\partial}{\partial \theta_1} + (\sin \theta_1)^{-2} \Delta_{\mathbb{S}^{d-1}}$$

where $\Delta_{\mathbb{S}^{d-1}}$ is the Laplace-Beltrami operator on the \mathbb{S}^{d-1} sphere parameterized by $\theta_2, \dots, \theta_d$.

For each $\ell \in \mathbb{N}$, $\nu_\ell := -\ell(\ell+d-1)$ is an eigenvalue of the Laplace-Beltrami operator. The corresponding eigenspace has an orthonormal basis of $N_\ell := \frac{(2\ell+d-1)\Gamma(\ell+d-1)}{\Gamma(\ell+1)\Gamma(d)}$ eigenfunctions, $\{Y_\ell^\mu\}_{\mu=1}^{N_\ell}$ *spherical harmonics* of degree ℓ . Thus

$$\Delta Y_\ell^\mu = \nu_\ell Y_\ell^\mu.$$

We denote the space of spherical harmonics of degree $\ell \leq m$ as

$$\Pi_m := \text{span}\{Y_\ell^\mu \mid \mu \leq N_\ell, \ell \leq m\} \quad (3)$$

and let $M := \dim \Pi_m = \frac{(2m+d)\Gamma(m+d)}{\Gamma(d+1)\Gamma(m+1)}$. The collection $(Y_\ell^\mu)_{\ell \geq 0, \mu \leq N_\ell}$ forms an orthonormal basis for $L_2(\mathbb{S}^d)$.

Operator Throughout this article we use \mathcal{L} to denote an operator (not differential, per se) of the form $\mathcal{L} = p(\Delta)$, where $p : \sigma(\Delta) \rightarrow \mathbb{R}$ is a function which grows at most algebraically. We define

$$\lambda_\ell := p(\nu_\ell),$$

and note that \mathcal{L} is diagonalized by spherical harmonics: $\mathcal{L}Y_\ell^\mu = \lambda_\ell Y_\ell^\mu$.

If p is a polynomial of degree k , then \mathcal{L} is a differential operator of order $2k$. The most elementary choices are the second order operators $\mathcal{L} = \Delta$ generated by $p(x) = x$ and $\mathcal{L} = 1 - \Delta$ generated by $p(x) = 1 - x$, but there are many higher order operators which arise in practice: $p(x) = x^2$ for the biharmonic, or $p(x) = 1 - x^2$ for the linear part of the Cahn-Hilliard equation as described in [22], or higher order powers of the Laplace-Beltrami $p(x) = \gamma x^j$ as considered for hyperviscosity terms added to differential operators in order to stabilize kernel-based methods for certain time-dependent PDEs [37].

Point sets For $\Omega \subset \mathbb{S}^d$ and finite subset $X \subset \Omega$, we define the *fill distance* of X in Ω as

$$h := \max_{x \in \Omega} \text{dist}(x, X) = \max_{x \in \Omega} \min_{x_j \in X} \text{dist}(x, x_j)$$

and the *separation radius* as

$$q := \frac{1}{2} \min_{x_j \in X} \min_{x_k \neq x_j} \text{dist}(x_j, x_k).$$

In general, the cardinality $N = \#X$ of X can be estimated above and below by $c_1 h^{-d} \leq N \leq c_2 q^{-d}$.

A family of point sets is called *quasi-uniform* if there is a constant ρ_0 so that for every X in the family, the ratio $\rho := h/q$ is bounded by ρ_0 . In this setting, one has $c_1 \rho^{-d} q^{-d} \leq N \leq c_2 q^{-d}$, and thus $q \sim N^{-1/d}$. Although most of our results hold for general point sets

without an a priori bound on the mesh ratio, some portions (in particular sections 4.4 and 5.1) make use of quasi-uniformity.

For numerical experiments, we employ some benchmark families of equi-distributed subsets of \mathbb{S}^2 for our numerical experiments in sections 4.5 and 5.2; namely, Fibonacci, minimum energy, maximum determinant, and Hammersley point sets (illustrated in Figure 2). The first three of these sets are quasi-uniform, with separation radii q that decay with the cardinality $N = \#X$ like $N^{-1/2}$, while the Hammersley points are highly unstructured; see [27] for more information on all of these point sets.

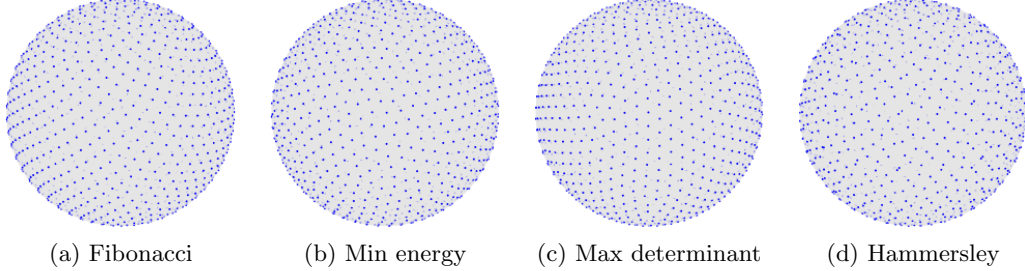


Figure 2: Examples from the point set families on \mathbb{S}^2 used in the numerical experiments. (a) has $N = 1025$ points, while for (b)–(d) have $N = 1024$ points.

Conditionally positive definite kernels We consider kernels $\Phi : \mathbb{S}^d \times \mathbb{S}^d \rightarrow \mathbb{R}$ which are *conditionally positive definite* (CPD) of order $\tilde{m} \in \mathbb{N}$ (i.e., CPD with respect to the spherical harmonic space $\Pi_{\tilde{m}-1}$). This means that for any point set $X \subset \mathbb{S}^2$, the *collocation matrix*

$$\Phi_X := (\Phi(x_j, x_k))_{j,k=1\dots N} = \begin{pmatrix} \Phi(x_1, x_1) & \dots & \Phi(x_1, x_N) \\ \vdots & \ddots & \vdots \\ \Phi(x_N, x_1) & \dots & \Phi(x_N, x_N) \end{pmatrix} \quad (4)$$

is strictly positive definite on the space of vectors

$$\left\{ \alpha \in \mathbb{R}^N \mid (\forall p \in \Pi_{\tilde{m}-1}) \sum_{j=1}^N \alpha_j p(x_j) = 0 \right\}.$$

A kernel is *positive definite* (PD) if for every X , the collocation matrix (4) is strictly PD on \mathbb{R}^N . Since such a kernel is CPD with respect to the trivial space $\Pi_{-1} = \{0\}$, for ease of exposition we use CPD of order $\tilde{m} = 0$ to mean PD.

For a given point set $X \subset \mathbb{S}^d$, define

$$S_X(\Phi) := \left\{ \sum_{j=1}^N a_j \Phi(\cdot, x_j) \mid (\forall p \in \Pi_{\tilde{m}-1}), \sum_{j=1}^N a_j p(x_j) = 0 \right\} + \Pi_{\tilde{m}-1}. \quad (5)$$

The kernels we consider in this paper are *zonal*, which means that they have a Mercer-like expansion

$$\Phi(x, y) = \sum_{\ell=0}^{\infty} \sum_{\mu \leq N_\ell} c_\ell Y_\ell^\mu(x) Y_\ell^\mu(y) \quad (6)$$

which is absolutely and uniformly convergent. By the addition theorem for spherical harmonics [32, Theorem 2], $\sum_{\mu \leq N_\ell} Y_\ell^\mu(x) Y_\ell^\mu(y) = \frac{N_\ell}{\text{vol}(\mathbb{S}^d)} P_\ell(x \cdot y)$, where P_ℓ is an algebraic polynomial of degree ℓ with $P_\ell(1) = 1$ and $|P_\ell(x)| \leq 1$ for all $-1 \leq x \leq 1$ by [32, Lemma

9].¹ It follows that a series of the form (6) converges uniformly and absolutely on $\mathbb{S}^d \times \mathbb{S}^d$ if and only if the coefficients c_ℓ satisfy

$$\frac{1}{\text{vol}(\mathbb{S}^d)} \sum_{\ell=0}^{\infty} |c_\ell| \frac{(2\ell + d - 1)\Gamma(\ell + d - 1)}{\Gamma(\ell + 1)\Gamma(d)} \sim \sum_{\ell=0}^{\infty} (1 + \ell^{d-1})|c_\ell| < \infty.$$

Here we have used the fact that $N_\ell = \frac{(2\ell+d-1)\Gamma(\ell+d-1)}{\Gamma(\ell+1)\Gamma(d)} \leq C_d \ell^{d-1}$ for $\ell \geq 1$ and for a d -dependent constant C_d .

Note that, by [31, Theorem 4.6], an expansion of the form (6) yields a kernel which is CPD of order \tilde{m} if and only if the expansion coefficients satisfy $c_\ell \geq 0$ for all $\ell \geq \tilde{m}$, and $c_\ell > 0$ for infinitely many odd and infinitely many even values of ℓ (the PD case (i.e., $\tilde{m} = 0$) was given in [8, Theorem 3]). However, most CPD kernels of interest have the property that $c_\ell > 0$ for all $\ell \geq \tilde{m}$. We direct the reader to [4] for a number of prominent examples of kernels (both PD and CPD) with precisely calculated coefficients c_ℓ .

Compatibility assumption between Φ and \mathcal{L} For a kernel Φ , and a differential operator \mathcal{L} , we adopt the convention that $\mathcal{L}\Phi(x, y)$ means that the operator is applied to the first argument, i.e., $\mathcal{L}\Phi(x, y) = \mathcal{L}^{(1)}\Phi(x, y)$.

The following assumption guarantees that Φ is CPD and that $\mathcal{L}\Phi$ is a zonal kernel. It is in force throughout this paper.

Assumption 2.1. *Let $\Phi : \mathbb{S}^d \times \mathbb{S}^d \rightarrow \mathbb{R}$ denote a kernel with a Mercer-like expansion (6), which is CPD of order $\tilde{m} \geq 0$ (where $\tilde{m} = 0$ means Φ is PD). Let $\mathcal{L} = p(\Delta)$ be a linear operator obtained by $p : \sigma(\Delta) \rightarrow \mathbb{R}$ so that the eigenvalues $\lambda_\ell = p(\nu_\ell)$ grow at most algebraically, and that $\sum_{\ell=0}^{\infty} c_\ell |\lambda_\ell| \ell^{d-1} < \infty$.*

Note that some of these assumptions have already been mentioned earlier in this section – the critical hypothesis is the compatibility condition between Φ and \mathcal{L} , namely $\sum_{\ell=0}^{\infty} c_\ell |\lambda_\ell| \ell^{d-1} < \infty$. This condition can be further simplified if \mathcal{L} is a differential operator of order $2L$ (in other words, if p is polynomial of degree L or less). The requirement that $\sum_{\ell=0}^{\infty} c_\ell |\lambda_\ell| \ell^{d-1}$ converges can be expressed in this case as $\sum_{\ell=0}^{\infty} c_\ell \ell^{2L+d-1} < \infty$.

Miscellaneous notation Throughout the paper, we let C (with or without subscripts) denote a generic positive constant. To denote matrices, we use bold upper case letters. We also use $\mathbf{A} \mapsto \|\mathbf{A}\|$ to denote the induced ℓ_2 matrix norm.

3 Spectral stability for PD kernels

If Assumption 2.1 holds with $\tilde{m} = 0$, we define the global DM \mathbf{M}_X for the finite point set $X \subset \mathbb{S}^d$ as the unique matrix in $\mathbb{R}^{N \times N}$ which satisfies the identity $\mathbf{M}_X \begin{pmatrix} u|_X \end{pmatrix} = (\mathcal{L}u)|_X$ for all $u \in S_X(\Phi)$. It has the form

$$\mathbf{M}_X = \mathbf{K}_X \Phi_X^{-1}, \quad (7)$$

where Φ_X is the collocation matrix (4) and

$$\mathbf{K}_X = \left(\mathcal{L}\Phi(x_j, x_k) \right)_{j,k}.$$

It follows that \mathbf{K}_X is a symmetric matrix generated by sampling $\Psi = \mathcal{L}\Phi$.

We can thus conclude that the spectrum of \mathbf{M}_X is the same as that of the symmetric matrix $\Phi_X^{-1/2} \mathbf{K}_X \Phi_X^{-1/2}$. In particular, if \mathcal{L} has non-negative spectrum (each $\lambda_\ell \geq 0$), then \mathbf{K}_X is positive semi-definite, so $\sigma(\mathbf{M}_X) \subset [0, \infty)$. Furthermore, if $\lambda_\ell c_\ell > 0$ for infinitely many odd and infinitely many even ℓ , then \mathbf{K}_X is strictly positive definite, and $\sigma(\mathbf{M}_X) \subset (0, \infty)$.

¹The functions P_ℓ are orthogonal with respect to the weight $(1 - x^2)^{\frac{d-2}{2}}$, and are thus proportional to a Gegenbauer polynomials $C_\ell^{(\frac{d-1}{2})}$ as defined in [1, Chapter 22].

3.1 Conditioning of the eigenbasis of \mathbf{M}_X

While the above setup shows that \mathbf{M}_X is diagonalizable and we have control on $\sigma(\mathbf{M}_X)$, the eigenvectors of \mathbf{M}_X may be far from orthogonal. To understand the conditioning of the eigenbasis of \mathbf{M}_X , we consider the matrix

$$\mathbf{N}_X := \Phi_X^{-1/2} \mathbf{M}_X \Phi_X^{1/2},$$

which, by the above factorization, satisfies $\mathbf{N}_X = \Phi_X^{-1/2} \mathbf{K}_X \Phi_X^{-1/2}$, and is therefore symmetric.

Proposition 3.1. *Suppose Assumption 2.1 holds with $\tilde{m} = 0$. If $X \subset \mathbb{S}^d$ has cardinality $\#X = N$ and if $\mathbf{M}^\epsilon \in \mathbb{R}^{N \times N}$ then for every eigenvalue λ^ϵ of \mathbf{M}^ϵ , there is an eigenvalue λ of \mathbf{M}_X with*

$$|\lambda - \lambda^\epsilon| \leq \text{cond}(\Phi_X^{1/2}) \|\mathbf{M}_X - \mathbf{M}^\epsilon\|$$

where $\text{cond}(\Phi_X^{1/2}) = \|\Phi_X^{1/2}\| \|\Phi_X^{-1/2}\|$ is the ℓ_2 condition number of $\Phi_X^{1/2}$.

Proof. By the above comment, $\mathbf{N}_X = \mathbf{U} \mathbf{D} \mathbf{U}^T$ with \mathbf{U} an orthogonal matrix. Hence, we have a diagonalization of the form

$$\mathbf{M}_X = \Phi_X^{1/2} \mathbf{N}_X \Phi_X^{-1/2} = \mathbf{V} \mathbf{D} \mathbf{V}^{-1}$$

with $\mathbf{V} := \Phi_X^{1/2} \mathbf{U}$. As \mathbf{U} is orthogonal, $\text{cond}(\mathbf{V}) = \|\mathbf{V}\| \|\mathbf{V}^{-1}\|$ satisfies

$$\text{cond}(\mathbf{V}) \leq \|\Phi_X^{1/2}\| \|\Phi_X^{-1/2}\| \|\mathbf{U}\| \|\mathbf{U}^{-1}\| = \text{cond}(\Phi_X^{1/2}).$$

The result then follows by an application of the Bauer-Fike theorem [3]. \square

In case Φ has coefficients which have prescribed algebraic decay $c_\ell \sim |\nu_\ell|^{-m}$, it is possible to control the smallest eigenvalue of the collocation matrix by a power of the separation radius q . This situation corresponds to a number of kernels with Sobolev native spaces, including compactly supported kernels and restricted Matérn kernels, as described in [12, Appendix].

Corollary 3.2. *Suppose the hypotheses of Proposition 3.1 hold, and the expansion coefficients c_ℓ of Φ satisfy $c_\ell \sim |\nu_\ell|^{-m}$. Then for every eigenvalue λ^ϵ of \mathbf{M}^ϵ , there is an eigenvalue λ of \mathbf{M}_X with*

$$|\lambda - \lambda^\epsilon| \leq Cq^{-m} \|\mathbf{M}_X - \mathbf{M}^\epsilon\|.$$

Proof. By [12, Lemma 4.2], the decay of the coefficients c_ℓ allows us to bound $\|\Phi_X^{-1/2}\|$ by $Cq^{d/2-m}$, while $\|\Phi_X^{1/2}\| \leq \|\Phi_X\|^{1/2} \leq Cq^{-d/2}$ since Φ is bounded and $N \leq Cq^{-d}$. Thus

$$\text{cond}(\Phi_X^{1/2}) \leq Cq^{-m}$$

and the corollary follows. \square

Note that if $c_\ell \sim |\nu_\ell|^{-m}$ and p is a polynomial of degree L or less, so \mathcal{L} is a differential operator of order $2L$, then the summability condition $\sum_{\ell=0}^{\infty} c_\ell |\lambda_\ell| \ell^{d-1} < \infty$ from Assumption 2.1 is equivalent to $L < m - d/2$.

3.2 Generalizations to other settings

The above setup can be generalized considerably to other manifolds \mathbb{M} and operators \mathcal{L} . We begin by assuming that the underlying set \mathbb{M} is a metric space with distance function $\text{dist} : \mathbb{M} \times \mathbb{M} \rightarrow [0, \infty)$.

If $\phi_j : \mathbb{M} \rightarrow \mathbb{R}$ is one of a countable collection of continuous functions whose span is dense in $C(\mathbb{M})$ then any series

$$\Phi(x, y) = \sum_{j=0}^{\infty} c_j \phi_j(x) \phi_j(y) \quad (8)$$

which converges absolutely and uniformly is PD if $c_j > 0$ for every j . In particular, the collocation matrix $\Phi_X = (\Phi(x_j, x_k))_{j,k}$ is positive definite for any finite set $X \subset \mathbb{M}$.

If \mathcal{L} is a linear operator diagonalized by the ϕ_j 's, i.e., $\lambda_j \phi_j = \mathcal{L} \phi_j$ and for which the series $\Psi(x, y) = \sum_j c_j \lambda_j \phi_j(x) \phi_j(y)$ converges absolutely and uniformly, then the DM has the form $\mathbf{M}_X = \mathbf{K}_X \Phi_X^{-1}$ where $\mathbf{K}_X = (\Psi(x_j, x_k))_{j,k}$ is symmetric, and the perturbation result of Proposition 3.1 holds in this setting.

Example 1: (intrinsic) compact Riemannian Manifolds A common setup involves a compact, d -dimensional Riemannian manifold (\mathbb{M}, g) endowed with Laplace-Beltrami operator, given in intrinsic coordinates as

$$\Delta_{\mathbb{M}} = \frac{1}{\sqrt{\det g(x)}} \sum_{j,k} \frac{\partial}{\partial x_k} \left(\sqrt{\det g(x)} g^{jk} \frac{\partial}{\partial x_j} \right).$$

In this case, there exists a countable orthonormal basis (ϕ_j) of eigenvectors of \mathcal{L} with corresponding eigenvalues $\dots \leq \nu_1 < \nu_0 = 0$. We may assume each ϕ_j to be real-valued.

In this setting, we may again let $\mathcal{L} = p(\Delta)$ for a function defined on $\sigma(\Delta_{\mathbb{M}})$. The requirement of absolute and uniform convergence of the series $\sum_{j=1}^{\infty} \lambda_j c_j \phi_j(x) \phi_j(y)$ may be simplified by using Weyl laws to control the growth of $|\nu_j|$. Estimates in the uniform norm of eigenfunctions can be obtained in specific cases, see e.g. [39, Theorem 2.1] or [11].

There are two immediate challenges to this approach. The first comes purely from adapting Corollary 3.2. In order to estimate the condition number of the eigenbasis in terms of the separation radius q . As in the case $\mathbb{M} = \mathbb{S}^d$, this can be controlled by estimating the minimal eigenvalue of the collocation matrix Φ_X . To control this eigenvalue one may attempt to adapt [12, Lemma 4.2], although the much more general spectral theoretic arguments of [23], specifically [23, Proposition 8] may be more easily adapted to this setting.

The second challenge stems from using the kernel Φ and the DM \mathbf{M}_X . Although nicely defined by a series, the kernel Φ may not have a convenient closed-form representation. This challenge can be addressed if the eigenfunctions ϕ_j appearing in (8) are known. If this is the case, it may be suitable to truncate the Mercer-like series at a sufficiently large threshold N . Of course, truncating the kernel imposes some error which would need to be managed (for instance by way of perturbation results like Corollary 3.2).

Example 2: embedded compact Riemannian Manifolds If $\mathbb{M} \subset \mathbb{R}^{d+k}$ is a compact Riemannian manifold embedded in Euclidean space, we may follow [18] by considering a radial basis function (RBF) $\varphi : \mathbb{R}^{d+k} \rightarrow \mathbb{R}$, namely a function which is symmetric under rotations (i.e., $\varphi(x) = \tau(|x|)$ for some function $\tau : [0, \infty) \rightarrow \mathbb{R}$) and has Fourier transform which satisfies $C_1(1 + |\xi|^2)^{-m} \leq \widehat{\varphi}(\xi) \leq C_2(1 + |\xi|^2)^{-m}$ for some $0 < C_1 \leq C_2 < \infty$.

In that case, $\Phi : \mathbb{M} \times \mathbb{M} \rightarrow \mathbb{R} : (x, y) \mapsto \varphi(x - y)$ is a PD kernel on \mathbb{M} . By Mercer's theorem, it has an absolutely and uniformly convergent expansion of the form (8), where the functions ϕ_j are eigenfunctions of the integral operator $f \mapsto \int_{\mathbb{M}} f(x) \Phi(\cdot, x) dx$.

The challenge in this case is that closed form expressions for the eigenfunctions ϕ_j 's and coefficients c_j are not known in general (see [36] for an approach to approximate these). As a result, it is difficult to identify the operators \mathcal{L} diagonalized by ϕ_j which are necessary to apply Proposition 3.1.

In contrast to the case of Example 1, [43, Theorem 12.3] guarantees that the collocation matrix Φ_X has minimal eigenvalue $\lambda_{\min}(\Phi_X) \geq Cq^{2m-(d+k)/2}$, so $\|\Phi_X^{-1}\| \leq Cq^{(d+k)/2-2m}$.

On the other hand $\|\Phi_X\|_2 \leq \sqrt{N}\|\Phi\|_\infty \leq Cq^{-d/2}$ is guaranteed by the continuity of Φ and the compactness of \mathbb{M} , so an analogue of Corollary 3.2 holds in this case with estimate

$$|\lambda - \lambda^\epsilon| \leq Cq^{k/2-m}\|\mathbf{M}_X - \mathbf{M}^\epsilon\|.$$

4 Spectral stability for CPD kernels

We now present our main results for global DMs constructed using CPD kernels. In section 4.1 we show that \mathbf{M}_X is similar to the sum of a diagonal matrix and nilpotent matrix with a single nonzero $(1, 2)$ block. This is Lemma 4.1. In section 4.2 we give a preliminary version of the Bauer-Fike theorem which treats the block triangular factorization. Section 4.3 considers the full diagonalization of \mathbf{M}_X under mild assumptions on the operator \mathcal{L} . We analyze the norms of various factors appearing in the factorization in Section 4.4.

4.1 DM block decomposition

For a CPD kernel Φ of order $\tilde{m} > 0$ and operator \mathcal{L} which satisfy Assumption 2.1, and for a point set $X \subset \mathbb{S}^d$, define the DM \mathbf{M}_X so that $\mathbf{M}_X(u|_X) = (\mathcal{L}u)|_X$ holds for all $u \in S_X(\Phi)$. Then \mathbf{M}_X can be expressed as

$$\mathbf{M}_X = (\mathcal{L}\chi_j(x_k))_{j,k} = \mathbf{K}_X \mathbf{A} + \mathbf{P} \mathbf{A} \mathbf{B}, \quad (9)$$

where $\mathbf{K}_X = (\mathcal{L}\Phi(x_j, x_k))_{j,k}$ and $\mathbf{P} = (p_j(x_k))_{j \leq M}$ is an $N \times M$ Vandermonde matrix associated with a basis $\{p_j\}$ for $\Pi_{\tilde{m}-1}$ (see (3)). Here we take $p_j = Y_\ell^\mu$, for a suitable enumeration $(\ell, \mu) \leftrightarrow j$, so that \mathbf{A} is the diagonal matrix such that $\mathbf{P} \mathbf{A} = (\lambda_\ell p_j(x_k))_{k,j}$. The matrices \mathbf{A} and \mathbf{B} occur as solutions to the augmented kernel collocation problem

$$\begin{pmatrix} \Phi_X & \mathbf{P} \\ \mathbf{P}^T & \mathbf{0} \end{pmatrix} \begin{pmatrix} \mathbf{A} \\ \mathbf{B} \end{pmatrix} = \begin{pmatrix} \mathbf{I}_N \\ \mathbf{0} \end{pmatrix}, \quad (10)$$

where $\Phi_X := (\Phi(x_j, x_k))_{j,k}$ is the kernel collocation matrix. The kernel collocation matrix is a saddle-point matrix and we will exploit this structure and known facts for those matrices as they can be found for instance in [6] later on.

Let $\mathbf{P}^\dagger := (\mathbf{P}^T \mathbf{P})^{-1} \mathbf{P}^T$ be the standard left inverse of \mathbf{P} and $\mathbf{Q} = \mathbf{I}_N - \mathbf{P} \mathbf{P}^\dagger$ be the orthogonal projector onto the space $(\text{range}(\mathbf{P}))^\perp$ where

$$(\text{range}(\mathbf{P}))^\perp = \Pi_{\tilde{m}-1}(X)^\perp = \left\{ a \in \mathbb{R}^N \mid \sum_{j=1}^N a_j p(x_j) \text{ for all } p \in \Pi_{\tilde{m}-1}(\mathbb{R}^d) \right\}.$$

Let $\mathbf{W} \in \mathbb{R}^{N \times (N-M)}$ be a matrix whose columns form an orthonormal basis for $\Pi_{\tilde{m}-1}(X)^\perp$. Then $\mathbf{W} \mathbf{W}^T = \mathbf{Q}$.

By [6, (3.8)], we can write

$$\mathbf{A} = \mathbf{W} (\mathbf{W}^T \Phi_X \mathbf{W})^{-1} \mathbf{W}^T \quad (11)$$

$$\mathbf{B} = \mathbf{P}^\dagger (\mathbf{I}_N - \Phi_X \mathbf{A}). \quad (12)$$

The first equation shows that \mathbf{A} is positive semi-definite and that

$$\mathbf{A} = \mathbf{Q} \mathbf{A} \mathbf{Q} = \mathbf{A} \mathbf{Q} = \mathbf{Q} \mathbf{A}. \quad (13)$$

From (12), we can begin to decompose \mathbf{M}_X , obtaining first

$$\begin{aligned} \mathbf{M}_X &= \mathbf{K}_X \mathbf{A} + \mathbf{P} \mathbf{A} \mathbf{P}^\dagger (\mathbf{I}_N - \Phi_X \mathbf{A}) \\ &= \mathbf{P} \mathbf{A} \mathbf{P}^\dagger + (\mathbf{K}_X - \mathbf{P} \mathbf{A} \mathbf{P}^\dagger \Phi_X) \mathbf{A}. \end{aligned} \quad (14)$$

Adding and subtracting $\mathbf{P}\mathbf{P}^\dagger\mathbf{K}_X$, we write the second term in (14) as

$$(\mathbf{K}_X - \mathbf{P}\mathbf{A}\mathbf{P}^\dagger\mathbf{\Phi}_X)\mathbf{A} = (\mathbf{K}_X - \mathbf{P}\mathbf{P}^\dagger\mathbf{K}_X)\mathbf{A} + \mathbf{P}(\mathbf{P}^\dagger\mathbf{K}_X - \mathbf{A}\mathbf{P}^\dagger\mathbf{\Phi}_X)\mathbf{A}.$$

The first term in this expression is $\mathbf{Q}\mathbf{K}_X\mathbf{A}$, which equals $\mathbf{Q}\mathbf{K}_X\mathbf{A}\mathbf{Q}$ by (13). This gives the identity:

$$\mathbf{M}_X = \mathbf{P}\mathbf{A}\mathbf{P}^\dagger + \mathbf{Q}\mathbf{K}_X\mathbf{A}\mathbf{Q} + \mathbf{P}(\mathbf{P}^\dagger\mathbf{K}_X - \mathbf{A}\mathbf{P}^\dagger\mathbf{\Phi}_X)\mathbf{A}. \quad (15)$$

The first term in (15) corresponds to a diagonalizable block. Indeed, restricting \mathbf{M}_X to the invariant subspace $\Pi_{\tilde{m}-1}(X)$ yields $\mathbf{M}_X v = \mathbf{P}\mathbf{A}\mathbf{P}^\dagger v$ for $v \in \Pi_{\tilde{m}-1}(X)$.

The second term in (15) can also be viewed as a block of \mathbf{M}_X , this time restricted to $\Pi_{\tilde{m}-1}(X)^\perp$ (recall that \mathbf{A} annihilates $\Pi_{\tilde{m}-1}(X)$). Indeed, $\mathbf{Q}\mathbf{K}_X\mathbf{A}\mathbf{Q}$ can be diagonalized, as we did in section 3.1. This can be made more explicit with a change of basis using \mathbf{W} .

Change of basis For a matrix $\mathbf{C} \in \mathbb{R}^{N \times N}$, let

$$\widehat{\mathbf{C}} := \mathbf{W}^T \mathbf{C} \mathbf{W} \in \mathbb{R}^{(N-M) \times (N-M)} \quad (16)$$

Recall that the columns of \mathbf{W} form an orthonormal basis for $\Pi_{\tilde{m}-1}(X)^\perp$. Thus $\widehat{\mathbf{\Phi}}_X = \mathbf{W}^T \mathbf{\Phi}_X \mathbf{W}$ and its inverse $\widehat{\mathbf{A}} = \mathbf{W}^T \mathbf{A} \mathbf{W} = (\mathbf{W}^T \mathbf{\Phi}_X \mathbf{W})^{-1}$ are both positive definite.

By the same reasoning, $\widehat{\mathbf{K}}_X = \mathbf{W}^T \mathbf{K}_X \mathbf{W}$ is symmetric, and if $\lambda_\ell c_\ell \geq 0$ for $\ell \geq \tilde{m}$, then $\widehat{\mathbf{K}}_X$ is positive semi-definite. If, in addition, $\lambda_\ell c_\ell \neq 0$ for infinitely many even values of ℓ and infinitely many odd values of ℓ , then [31, Theorem 4.6] guarantees that $\widehat{\mathbf{K}}_X$ is strictly positive definite (this occurs, for instance, if $\mathcal{L} = p(\Delta)$ and p is a polynomial).

This yields the following result.

Lemma 4.1. *If Assumption 2.1 holds with $\tilde{m} > 0$ and $X \subset \mathbb{S}^d$ is finite, then the DM \mathbf{M}_X has factorization*

$$\mathbf{M}_X = \mathbf{V} \begin{pmatrix} \mathbf{\Lambda} & \mathbf{R} \\ \mathbf{0} & \mathbf{\Theta} \end{pmatrix} \mathbf{V}^{-1}$$

where $\mathbf{\Theta} \in \mathbb{R}^{(N-M) \times (N-M)}$ and $\mathbf{\Lambda} \in \mathbb{R}^{M \times M}$ are diagonal, and each entry $\Lambda_{j,j}$ is determined by the spectrum of \mathcal{L} on $\Pi_{\tilde{m}-1}$; i.e., with $\Lambda_{j,j} = \lambda_\ell$ where $p_j = Y_\ell^\mu$.

If $\lambda_\ell c_\ell \geq 0$ for all $\ell \geq \tilde{m}$, then each diagonal entry of $\mathbf{\Theta}$ is non-negative, and if, furthermore, $\lambda_\ell c_\ell \neq 0$ for infinitely many even and infinitely many odd values of ℓ , then each diagonal entry of $\mathbf{\Theta}$ is strictly positive.

Proof. The second term in (15) can be written as

$$\mathbf{Q}\mathbf{K}_X\mathbf{A}\mathbf{Q} = \mathbf{W}\widehat{\mathbf{K}}_X\widehat{\mathbf{A}}\mathbf{W}^T = \mathbf{W}\widehat{\mathbf{K}}_X\widehat{\mathbf{A}}\mathbf{W}^T, \quad (17)$$

since $\mathbf{K}_X\mathbf{A} = \mathbf{K}_X\mathbf{Q}\mathbf{A}$. Denote by

$$\mathbf{S} := (\widehat{\mathbf{A}})^{1/2} \in \mathbb{R}^{(N-M) \times (N-M)}$$

the symmetric positive definite square root of $\widehat{\mathbf{A}}$, i.e., $\widehat{\mathbf{A}} = \mathbf{S}^T \mathbf{S}$. By symmetry of $\mathbf{S}\widehat{\mathbf{K}}_X\mathbf{S}^T$, it follows that $\mathbf{S}\widehat{\mathbf{K}}_X\mathbf{S}^T = \mathbf{U}\mathbf{\Theta}\mathbf{U}^T$ for an orthogonal matrix $\mathbf{U} \in \mathbb{R}^{(N-M) \times (N-M)}$ and a diagonal matrix $\mathbf{\Theta} = \text{diag}(\theta_1, \dots, \theta_{N-M})$.

Hence, we have the factorization

$$\widehat{\mathbf{K}}_X\widehat{\mathbf{A}} = \mathbf{S}^{-1}(\mathbf{S}\widehat{\mathbf{K}}_X\mathbf{S}^T)\mathbf{S} = \mathbf{S}^{-1}\mathbf{U}\mathbf{\Theta}\mathbf{U}^T\mathbf{S}. \quad (18)$$

Define

$$\mathbf{Z} := \mathbf{W}\mathbf{S}^{-1}\mathbf{U} \in \mathbb{R}^{N \times (N-M)}. \quad (19)$$

Note that $\mathbf{U}^T \mathbf{S} \mathbf{W}^T$ is a left inverse of \mathbf{Z} . Writing $\mathbf{Z}^\dagger := \mathbf{U}^T \mathbf{S} \mathbf{W}^T$, we see that $\mathbf{Z} \mathbf{Z}^\dagger = \mathbf{Z}(\mathbf{U}^T \mathbf{S} \mathbf{W}^T) = \mathbf{W} \mathbf{W}^T = \mathbf{Q}$. Combining (17) and (18), we observe that $\mathbf{Q} \mathbf{K}_X \mathbf{A} \mathbf{Q} = \mathbf{W} \mathbf{S}^{-1} \mathbf{U} \Theta \mathbf{U}^T \mathbf{S} \mathbf{W}^T = \mathbf{Z} \Theta \mathbf{Z}^\dagger$, which yields

$$\mathbf{M}_X = \mathbf{P} \mathbf{A} \mathbf{P}^\dagger + \mathbf{Z} \Theta \mathbf{Z}^\dagger + \mathbf{P} \left(\mathbf{P}^\dagger \mathbf{K}_X - \Lambda \mathbf{P}^\dagger \Phi_X \right) \mathbf{A}. \quad (20)$$

Using $\mathbf{A} = \mathbf{A} \mathbf{Q} = \mathbf{A} \mathbf{Z} \mathbf{Z}^\dagger$, we have

$$\mathbf{P} \left(\mathbf{P}^\dagger \mathbf{K}_X - \Lambda \mathbf{P}^\dagger \Phi_X \right) \mathbf{A} = \mathbf{P} \mathbf{R} \mathbf{Z}^\dagger \quad (21)$$

with

$$\mathbf{R} := \left(\mathbf{P}^\dagger \mathbf{K}_X - \Lambda \mathbf{P}^\dagger \Phi_X \right) \mathbf{A} \mathbf{Z} \in \mathbb{R}^{M \times (N-M)}. \quad (22)$$

From (20), and (21), we have the factorization

$$\mathbf{M}_X = \begin{pmatrix} \mathbf{P} & \mathbf{Z} \end{pmatrix} \begin{pmatrix} \Lambda & \mathbf{R} \\ \mathbf{0} & \Theta \end{pmatrix} \begin{pmatrix} \mathbf{P}^\dagger \\ \mathbf{Z}^\dagger \end{pmatrix} \quad (23)$$

Finally, the square matrix matrix $\mathbf{V} := \begin{pmatrix} \mathbf{P} & \mathbf{Z} \end{pmatrix}$ satisfies

$$\begin{pmatrix} \mathbf{P} & \mathbf{Z} \end{pmatrix} \begin{pmatrix} \mathbf{P}^\dagger \\ \mathbf{Z}^\dagger \end{pmatrix} = \mathbf{P} \mathbf{P}^\dagger + \mathbf{Q} = \mathbf{I}_N$$

so $\mathbf{V}^{-1} = \begin{pmatrix} \mathbf{P}^\dagger & \mathbf{Z}^\dagger \end{pmatrix}^T$. By similarity, the spectrum of \mathbf{M}_X is

$$\sigma(\mathbf{M}_X) = \{\lambda_\ell \mid \ell < \tilde{m}\} \cup \{\theta_j \mid j \leq N - M\}.$$

Finally, we note that if $\lambda_\ell \geq 0$ for all $\ell \geq \tilde{m}$, then $\widehat{\mathbf{K}}_X$ is positive semi-definite, and so is $\widehat{\mathbf{S}} \widehat{\mathbf{K}}_X \widehat{\mathbf{S}}$. This implies that $\Theta = \mathbf{U}^T \widehat{\mathbf{S}} \widehat{\mathbf{K}}_X \widehat{\mathbf{S}}^T \mathbf{U}$, is positive semi-definite. Since Θ is diagonal, each $\theta_j \geq 0$. The last statement follows from the observation that $\widehat{\mathbf{K}}_X$ is positive definite in this case. \square

Remark 4.2. *As a consequence of Lemma 4.1 we obtain that $\sigma(\mathbf{M}_X) \subset (0, \infty)$ for an operator $\mathcal{L} = p(\Delta)$ with $p : \sigma(\Delta) \rightarrow (0, \infty)$ also for a CPD kernel of order \tilde{m} .*

More quantitative results will be shown in Lemma 4.4.

4.2 A generalization of the Bauer-Fike Theorem

By adapting the argument from [9], we obtain the following estimate on perturbation of eigenvalues of \mathbf{M}_X .

Proposition 4.3. *Under conditions of Lemma 4.1, if $\mathbf{M}^\epsilon \in \mathbb{R}^{N \times N}$ and if $\mu \in \sigma(\mathbf{M}^\epsilon)$, then*

$$\text{dist}(\mu, \sigma(\mathbf{M}_X)) \leq \max \left(2\kappa \|\mathbf{M}_X - \mathbf{M}^\epsilon\|, \sqrt{2\kappa \|\mathbf{R}\| \|\mathbf{M}_X - \mathbf{M}^\epsilon\|} \right)$$

holds with $\kappa := \text{cond}(\mathbf{V}) = \|\mathbf{V}\| \|\mathbf{V}^{-1}\|$. We note that \mathbf{R} and \mathbf{V} are matrices appearing in the decomposition of \mathbf{M}_X given in Lemma 4.1.

Proof. Assume without loss that $\mu \in \sigma(\mathbf{M}^\epsilon) \setminus \sigma(\mathbf{M}_X)$. For the invertible matrix \mathbf{V} given in (23), and for $\mathbf{E} := \mathbf{M}_X - \mathbf{M}^\epsilon$, we have the factorization

$$\begin{aligned} \mathbf{V}^{-1}(\mu \mathbf{I} - \mathbf{M}^\epsilon) \mathbf{V} &= \mu \mathbf{I} - \begin{pmatrix} \Lambda & \mathbf{R} \\ \mathbf{0} & \Theta \end{pmatrix} + \mathbf{V}^{-1} \mathbf{E} \mathbf{V} \\ &= \left(\mu \mathbf{I} - \begin{pmatrix} \Lambda & \mathbf{R} \\ \mathbf{0} & \Theta \end{pmatrix} \right) (\mathbf{I} + \tilde{\mathbf{E}}), \end{aligned}$$

where $\tilde{\mathbf{E}} := \left(\mu \mathbf{I} - \begin{pmatrix} \mathbf{\Lambda} & \mathbf{R} \\ 0 & \mathbf{\Theta} \end{pmatrix} \right)^{-1} \mathbf{V}^{-1} \mathbf{E} \mathbf{V}$. Since $\mathbf{V}^{-1}(\mu \mathbf{I} - \mathbf{M}^\epsilon) \mathbf{V}$ is singular and $\mu \notin \sigma(\mathbf{M}_X)$, it follows from the above factorization that $\mathbf{I} + \tilde{\mathbf{E}}$ is singular, and therefore we have that $\|\tilde{\mathbf{E}}\| \geq 1$. This ensures that

$$\left\| \left(\mu \mathbf{I} - \begin{pmatrix} \mathbf{\Lambda} & \mathbf{R} \\ 0 & \mathbf{\Theta} \end{pmatrix} \right)^{-1} \right\|^{-1} \leq \|\mathbf{V}^{-1} \mathbf{E} \mathbf{V}\| \leq \kappa \|\mathbf{M}_X - \mathbf{M}^\epsilon\|.$$

In other words,

$$\left\| \begin{pmatrix} \mu \mathbf{I}_M - \mathbf{\Lambda} & -\mathbf{R} \\ 0 & \mu \mathbf{I}_{N-M} - \mathbf{\Theta} \end{pmatrix}^{-1} \right\|^{-1} \leq \kappa(\mathbf{V}) \|\mathbf{M}_X - \mathbf{M}^\epsilon\|. \quad (24)$$

At this point, we may control the left hand side of (24) from below by estimating

$$\begin{aligned} F(\mu) &:= \left\| \begin{pmatrix} \mu \mathbf{I}_M - \mathbf{\Lambda} & -\mathbf{R} \\ 0 & \mu \mathbf{I}_{N-M} - \mathbf{\Theta} \end{pmatrix}^{-1} \right\| \\ &= \left\| \begin{pmatrix} (\mu \mathbf{I}_M - \mathbf{\Lambda})^{-1} & (\mu \mathbf{I}_M - \mathbf{\Lambda})^{-1} \mathbf{R} (\mu \mathbf{I}_{N-M} - \mathbf{\Theta})^{-1} \\ 0 & (\mu \mathbf{I}_{N-M} - \mathbf{\Theta})^{-1} \end{pmatrix} \right\|. \end{aligned}$$

By a triangle inequality:

$$\begin{aligned} F(\mu) &\leq \left\| \begin{pmatrix} (\mu \mathbf{I}_M - \mathbf{\Lambda})^{-1} & 0 \\ 0 & (\mu \mathbf{I}_{N-M} - \mathbf{\Theta})^{-1} \end{pmatrix} \right\| \\ &\quad + \left\| (\mu \mathbf{I}_M - \mathbf{\Lambda})^{-1} \mathbf{R} (\mu \mathbf{I}_{N-M} - \mathbf{\Theta})^{-1} \right\| \end{aligned}$$

Both $|(\mu - \Theta)_{j,j}^{-1}|$ and $|(\mu - \Lambda)_{k,k}^{-1}|$ can be controlled by $1/\text{dist}(\mu, \sigma(\mathbf{M}_X))$ for any $j \leq N - M$ and any $k \leq M$. Thus,

$$F(\mu) \leq (\text{dist}(\mu, \sigma(\mathbf{M}_X)))^{-1} + (\text{dist}(\mu, \sigma(\mathbf{M}_X)))^{-2} \|\mathbf{R}\|.$$

Case 1 If $(\text{dist}(\mu, \sigma(\mathbf{M}_X)))^{-1} \leq (\text{dist}(\mu, \sigma(\mathbf{M}_X)))^{-2} \|\mathbf{R}\|$, then the upper bound on $F(\mu)$ becomes $F(\mu) \leq 2(\text{dist}(\mu, \sigma(\mathbf{M}_X)))^{-2} \|\mathbf{R}\|$. So (24) guarantees that

$$\frac{(\text{dist}(\mu, \sigma(\mathbf{M}_X)))^2}{2\|\mathbf{R}\|} \leq \kappa \|\mathbf{M}_X - \mathbf{M}^\epsilon\|. \quad (25)$$

Case 2 If $(\text{dist}(\mu, \sigma(\mathbf{M}_X)))^{-1} > (\text{dist}(\mu, \sigma(\mathbf{M}_X)))^{-2} \|\mathbf{R}\|$, then the upper bound on $F(\mu)$ implies that $F(\mu) \leq 2(\text{dist}(\mu, \sigma(\mathbf{M}_X)))^{-1}$. So from (24) we have

$$\frac{(\text{dist}(\mu, \sigma(\mathbf{M}_X)))}{2} \leq \kappa \|\mathbf{M}_X - \mathbf{M}^\epsilon\|. \quad (26)$$

The result follows from (25) and (26). \square

4.3 Diagonalizing the DM

From Lemma 4.1 it follows that \mathbf{M}_X is diagonalizable if and only if $\begin{pmatrix} \mathbf{\Lambda} & \mathbf{R} \\ \mathbf{0} & \mathbf{\Theta} \end{pmatrix}$ is diagonalizable. We can recast this by way of the Sylvester problem: find $\mathbf{X} \in \mathbb{R}^{M \times (N-M)}$ so that

$$-\mathbf{\Lambda} \mathbf{X} + \mathbf{X} \mathbf{\Theta} = \mathbf{R}. \quad (27)$$

If (27) has a solution, then

$$\begin{pmatrix} \mathbf{\Lambda} & \mathbf{R} \\ \mathbf{0} & \mathbf{\Theta} \end{pmatrix} = \begin{pmatrix} \mathbf{I}_M & \mathbf{X} \\ \mathbf{0} & \mathbf{I}_{N-M} \end{pmatrix} \begin{pmatrix} \mathbf{\Lambda} & \mathbf{0} \\ \mathbf{0} & \mathbf{\Theta} \end{pmatrix} \begin{pmatrix} \mathbf{I}_M & -\mathbf{X} \\ \mathbf{0} & \mathbf{I}_{N-M} \end{pmatrix}, \quad (28)$$

so the block upper triangular matrix is diagonalizable. There are practical solution methods for problems of the form (27) under significantly more general conditions than we use (just the assumption that the spectra of $\sigma(\mathbf{\Lambda})$ and $\sigma(\mathbf{\Theta})$ are separated, see [2, 7] and [28] for an overview). In our case, where $\mathbf{\Lambda}$ and $\mathbf{\Theta}$ are diagonal, the solution is very simple.

We may rewrite (27) with the help of the matrix $\mathbf{\Gamma} = (\theta_j - \lambda_i)_{i,j}$. In that case, (27) has the form $\mathbf{\Gamma} \odot \mathbf{X} = \mathbf{R}$, where \odot is entry-wise multiplication. This leads to three cases:

1. The spectra of $\mathbf{\Lambda}$ and $\mathbf{\Theta}$ are disjoint, in which case $\mathbf{\Gamma}$ has no zero entries, and \mathbf{X} has a unique solution obtained by entry-wise division.
2. There is some overlap between spectra of $\mathbf{\Lambda}$ and $\mathbf{\Theta}$, but each zero entry of $\mathbf{\Gamma}$ corresponds to a zero entries of \mathbf{R} . In this case, there are many solutions to (27).
3. $\mathbf{\Theta}$ and $\mathbf{\Lambda}$, have overlapping spectra and $\mathbf{R}_{i,j} \neq 0$ for some i, j for which $\mathbf{\Gamma}_{j,j} = 0$. In this case, $\mathbf{\Lambda}_{i,i} = \mathbf{\Theta}_{j,j}$ has a generalized eigenvector.

If either case 1. or 2. holds, then (27) has a solution

Under basic hypotheses on the operator \mathcal{L} , we can estimate the separation between $\sigma(\mathbf{\Lambda})$ and $\sigma(\mathbf{\Theta})$, and therefore we can estimate the norm of \mathbf{X} .

Lemma 4.4. *Suppose Assumption 2.1 holds. Define numbers $\lambda_b, \lambda^\sharp \in \mathbb{R}$ as*

$$\lambda_b := \max\{p(\nu_\ell) \mid \ell < \tilde{m}\} \quad \text{and} \quad \lambda^\sharp := \min\{p(\nu_\ell) \mid \ell \geq \tilde{m}\}.$$

If $\lambda_b < \lambda^\sharp$, then $\min_{j \leq N-M} \mathbf{\Theta}_{j,j} - \max_{i \leq M} \mathbf{\Lambda}_{i,i} \geq \lambda^\sharp - \lambda_b > 0$.

Proof. Set $\tilde{\mathcal{L}} := \mathcal{L} - \lambda^\sharp \text{Id}$. Then $\tilde{\Psi} = \tilde{\mathcal{L}}\Phi$ is a zonal kernel and, moreover, is CPD of order \tilde{m} . By definition, $\Psi - \tilde{\Psi} = \lambda^\sharp \Phi$.

For $X \subset \mathbb{S}^d$, let $\mathbf{K}_X := (\Psi(x_j, x_k))_{j,k}$ and $\tilde{\mathbf{K}}_X := (\tilde{\Psi}(x_j, x_k))_{j,k}$. Both matrices are symmetric, and we have that $\tilde{\mathbf{K}}_X = \mathbf{K}_X - \lambda^\sharp \Phi_X$. Define $\tilde{\mathbf{\Lambda}} := \mathbf{\Lambda} - \lambda^\sharp \mathbf{I}_M$, and note that $\tilde{\mathbf{\Lambda}}$ satisfies the property that $\mathbf{P}\tilde{\mathbf{\Lambda}} = \mathbf{P}\mathbf{\Lambda} - \lambda^\sharp \mathbf{P}$. Thus the DM for $\tilde{\mathcal{L}}$ is

$$\tilde{\mathbf{M}}_X = \tilde{\mathbf{K}}_X \mathbf{A} + \mathbf{P}\tilde{\mathbf{\Lambda}}\mathbf{B} = \mathbf{M}_X - \lambda^\sharp \mathbf{I}_N.$$

From Lemma 4.1, it follows that $\tilde{\mathbf{M}}_X$ has spectrum

$$\sigma(\tilde{\mathbf{M}}_X) = \{p(\nu_\ell) - \lambda^\sharp \mid \ell < \tilde{m}\} \cup \{\tilde{\theta}_j \mid j \leq N - M\},$$

and that the first component satisfies the inclusion

$$\{\lambda_\ell - \lambda^\sharp \mid \ell < \tilde{m}\} \subset (-\infty, \lambda_b - \lambda^\sharp] \subset (-\infty, 0)$$

while $\{\tilde{\theta}_j \mid j \leq N - M\} \subset [0, \infty)$. Thus, for \mathbf{M}_X , the DM for \mathcal{L} , we have the disjoint union

$$\sigma(\mathbf{M}_X) = \sigma(\tilde{\mathbf{M}}_X) + \lambda^\sharp = \{\lambda_\ell \mid \ell < \tilde{m}\} \sqcup \{\theta_j \mid j \leq N - M\}.$$

□

In case the hypotheses of Lemma 4.4 hold, we can diagonalize \mathbf{M}_X and make use of the standard Bauer-Fike theorem instead of Proposition 4.3.

Theorem 4.5. *Suppose Assumption 2.1 holds with $\tilde{m} > 0$. If the separation*

$$\gamma := \min_{\ell \geq \tilde{m}} \lambda_\ell - \max_{\ell < \tilde{m}} \lambda_\ell$$

is positive, then for any N -set $X \subset \mathbb{S}^d$, \mathbf{M}_X is diagonalizable, and for matrix $\mathbf{M}^\epsilon \in \mathbb{R}^{N \times N}$ and eigenvalue $\mu \in \sigma(\mathbf{M}^\epsilon)$ we have

$$\text{dist}(\mu, \sigma(\mathbf{M}_X)) \leq \left(1 + \frac{\|\mathbf{R}\|}{\gamma}\right)^2 \|\mathbf{V}\| \|\mathbf{V}^{-1}\| \|\mathbf{M}_X - \mathbf{M}^\epsilon\|.$$

Here \mathbf{R} and \mathbf{V} are matrices appearing in the decomposition of \mathbf{M}_X given in Lemma 4.1.

Proof. From Lemma 4.1 and (28), \mathbf{M}_X has the factorization:

$$\mathbf{M}_X = \tilde{\mathbf{V}} \begin{pmatrix} \mathbf{\Lambda} & \mathbf{0} \\ \mathbf{0} & \mathbf{\Theta} \end{pmatrix} \tilde{\mathbf{V}}^{-1} \quad \text{where} \quad \tilde{\mathbf{V}} := \mathbf{V} \begin{pmatrix} \mathbf{I}_M & \mathbf{X} \\ \mathbf{0} & \mathbf{I}_{N-M} \end{pmatrix}$$

and where $\mathbf{\Gamma} \odot \mathbf{X} = \mathbf{R}$. The condition number for the eigenbasis is controlled by $\kappa(\tilde{\mathbf{V}}) \leq (1 + \|\mathbf{X}\|)^2 \|\mathbf{V}\| \|\mathbf{V}^{-1}\|$. We can estimate $\|\mathbf{X}\| \leq \frac{1}{\gamma} \|\mathbf{R}\|$. The result then follows from the standard Bauer-Fike theorem. \square

4.4 Matrix norms of elements of the block decomposition

We now restrict the situation to kernels which are CPD of order \tilde{m} and for which the coefficients in the expansion (6) satisfy $c_\ell \sim |\nu_\ell|^{-m}$ for all $\ell \geq \tilde{m}$.

Estimating $\|\mathbf{P}\|$ and $\|\mathbf{P}^\dagger\|$ We can estimate $\|\mathbf{P}\|$ via Hölder's inequality.

$$\sum_{k \leq M} \left| \sum_{j \leq N} a_j p_j(x_k) \right|^2 \leq \sum_{k \leq M} \|a\|_2^2 \sum_{j \leq N} |p_j(x_k)|^2 \leq NM \max_{j \leq M} \|p_j\|_\infty^2 \|a\|_2^2,$$

so $\|\mathbf{P}\| \leq \sqrt{NM} \max_{j \leq M} \|p_j\|_\infty$. Since M is assumed to be fixed and $N \leq Cq^{-d}$, we can express this estimate as

$$\|\mathbf{P}\| \leq Cq^{-d/2}. \quad (29)$$

Naturally, the bound (29) holds for $\|\mathbf{P}^T\|$ as well.

A simple consequence of [33, Theorem 4.2] guarantees that the Gram matrix $\mathbf{P}^T \mathbf{P}$ has spectrum contained in the interval $[C_1 h^{-d}, C_2 q^{-d}]$ for constants C_1 and C_2 independent of X (see [12, Lemma 4.2] for this argument in the case $d = 2$). It follows that $\|(\mathbf{P}^T \mathbf{P})^{-1}\| \leq Ch^d \leq C\rho^d q^d$, where $\rho = h/q$ is the *mesh ratio* of X , and C is a constant that only depends on \tilde{m} and d . Thus,

$$\|\mathbf{P}^\dagger\| \leq \|(\mathbf{P}^T \mathbf{P})^{-1}\| \|\mathbf{P}^T\| \leq C\rho^d q^{d/2}. \quad (30)$$

Estimating $\|\mathbf{Z}\|$ and $\|\mathbf{Z}^\dagger\|$ By [17, Proposition 5.2], the minimal eigenvalue λ_{\min} of $\mathbf{W}^T \mathbf{\Phi}_X \mathbf{W}$ is bounded below by $\lambda_{\min} \geq C_1 q^{2m-d}$ for some constant $C_1 > 0$.

Additionally, since \mathbf{S} is the positive square root of $\hat{\mathbf{A}}$ and

$$\|\mathbf{S}\| = \|\hat{\mathbf{A}}^{1/2}\| = \|\hat{\mathbf{A}}\|^{1/2} = \|(\mathbf{W}^T \mathbf{\Phi} \mathbf{W})^{-1}\|^{1/2} \leq Cq^{d/2-m}$$

we have, since $\mathbf{Z}^\dagger = \mathbf{U}^T \mathbf{S} \mathbf{W}^T$, that

$$\|\mathbf{Z}^\dagger\| = \|\mathbf{S}\| \leq Cq^{d/2-m}.$$

From (19) we know $\|\mathbf{Z}\| = \|\mathbf{S}^{-1}\|$, so it follows that

$$\|\mathbf{Z}\| = \|\mathbf{S}^{-1}\| = \|\hat{\mathbf{A}}^{-1/2}\| = \|\mathbf{W}^T \mathbf{\Phi}_X \mathbf{W}\|^{1/2} \leq \|\mathbf{\Phi}_X\|^{1/2}.$$

By the estimate $\|\mathbf{\Phi}_X\| \leq \|\mathbf{\Phi}\|_\infty N$, we have

$$\|\mathbf{Z}\| \leq Cq^{-d/2}.$$

Estimating $\|\mathbf{R}\|$ Treating perturbations of the kernel DM in the CPD case requires handling the upper right hand block \mathbf{R} in the decomposition (23).

To estimate $\|\mathbf{R}\| = \left\| \left(\mathbf{P}^\dagger \mathbf{K}_X - \Lambda \mathbf{P}^\dagger \Phi_X \right) \mathbf{A} \mathbf{Z} \right\|$, note that

- $\|\mathbf{Z}\| \leq Cq^{-d/2}$;
- $\|\mathbf{A}\| = \|\widehat{\mathbf{A}}\| \leq Cq^{d-2m}$ by (11);
- $\|\mathbf{P}^\dagger \mathbf{K}_X\| \leq \|\mathbf{P}^\dagger\| \|\mathbf{K}_X\| \leq C\rho^d q^{-d/2}$;
- $\|\Lambda \mathbf{P}^\dagger \Phi_X\| \leq (\max_{\ell < \tilde{m}} \lambda_\ell) \|\mathbf{P}^\dagger\| \|\Phi_X\| \leq C\rho^d q^{-d/2}$.

The latter two use the matrix norms $\|\mathbf{K}_X\|$ and $\|\Phi_X\|$, which can be estimated by introducing supremum norms $\|\Phi\|_\infty = \max_{x,y} |\Phi(x,y)|$ and $\|\mathcal{L}\Phi\|_\infty = \max_{x,y} |\mathcal{L}\Phi(x,y)|$, to obtain $\|\Phi_X\| \leq N\|\Phi\|_\infty$ and $\|\mathbf{K}_X\| \leq N\|\mathcal{L}\Phi\|_\infty$. Recalling that $N \leq Cq^{-d}$, we obtain the bound

$$\|\mathbf{R}\| \leq C\rho^d q^{-d/2} q^{d-2m} q^{-d/2} \leq C\rho^d q^{-2m}. \quad (31)$$

It is conceivable that a much better estimate is possible, since the factor $\mathbf{P}^\dagger \mathbf{K}_X - \Lambda \mathbf{P}^\dagger \Phi_X$, which involves a commutator-like factor (namely $\mathbf{P}^\dagger \mathcal{L} - \mathcal{L} \mathbf{P}^\dagger$), has been roughly estimated with a triangle inequality. We investigate this numerically in the next section.

Estimating the condition number of \mathbf{V} We now consider the condition number $\kappa = \text{cond}(\mathbf{V}) = \|\mathbf{V}\| \|\mathbf{V}^{-1}\|$ appearing in Lemma 4.3.

The blocks \mathbf{P} and \mathbf{Z} of $\mathbf{V} = \begin{pmatrix} \mathbf{P} & \mathbf{Z} \end{pmatrix}$ have orthogonal ranges and nullspaces. Indeed, we have

$$\text{Range } \mathbf{P} = \Pi_{\tilde{m}-1}(X) = \text{Null } \mathbf{Q} = \text{Null } \mathbf{W}^T = \text{Null } \mathbf{Z}^\dagger$$

and

$$\text{Range } \mathbf{Z} = (\Pi_{\tilde{m}-1}(X))^\perp = \text{Range } \mathbf{W} = \text{Range } \mathbf{Q} = \text{Null } \mathbf{P}^\dagger.$$

Thus, $\|\mathbf{V}\| \leq \max(\|\mathbf{P}\|, \|\mathbf{Z}\|)$ and $\|\mathbf{V}^{-1}\| \leq \max(\|\mathbf{P}^\dagger\|, \|\mathbf{Z}^\dagger\|)$. It follows that

$$\|\mathbf{V}\| \leq \max(\|\mathbf{P}\|, \|\mathbf{Z}\|) \leq Cq^{-d/2}$$

If $c_\ell \sim |\nu_\ell|^{-m}$, we have

$$\|\mathbf{V}^{-1}\| \leq \max(\|\mathbf{P}^\dagger\|, \|\mathbf{Z}^\dagger\|) \leq Cq^{d/2} \max(\rho^d, q^{-m}).$$

Together, this implies

$$\kappa \leq C \max(\rho^d, q^{-m}).$$

Corollary 4.6. *Under hypotheses of Proposition 4.3, if we assume the kernel's expansion coefficients c_ℓ satisfy $c_\ell \sim |\nu_\ell|^{-m}$ for all $\ell \geq \tilde{m}$ and $\rho \lesssim q^{-m/d}$, then for a matrix \mathbf{M}^ϵ sufficiently close to \mathbf{M}_X , and $\mu \in \sigma(\mathbf{M}^\epsilon)$ there is a $\lambda \in \sigma(\mathbf{M}_X)$ for which*

$$\begin{aligned} |\mu - \lambda| &\leq C \max \left(q^{-m/2} \|\mathbf{R}\|^{1/2} \sqrt{\|\mathbf{M} - \mathbf{M}^\epsilon\|}, q^{-m} \|\mathbf{M} - \mathbf{M}^\epsilon\| \right) \\ &\leq Cq^{-3m/2} \sqrt{\|\mathbf{M}_X - \mathbf{M}^\epsilon\|}. \end{aligned}$$

Proof. Plugging the estimate $\kappa \leq Cq^{-m}$ into Proposition 4.3 gives the first inequality. Using the bound (31) for $\|\mathbf{R}\|$ gives the second. \square

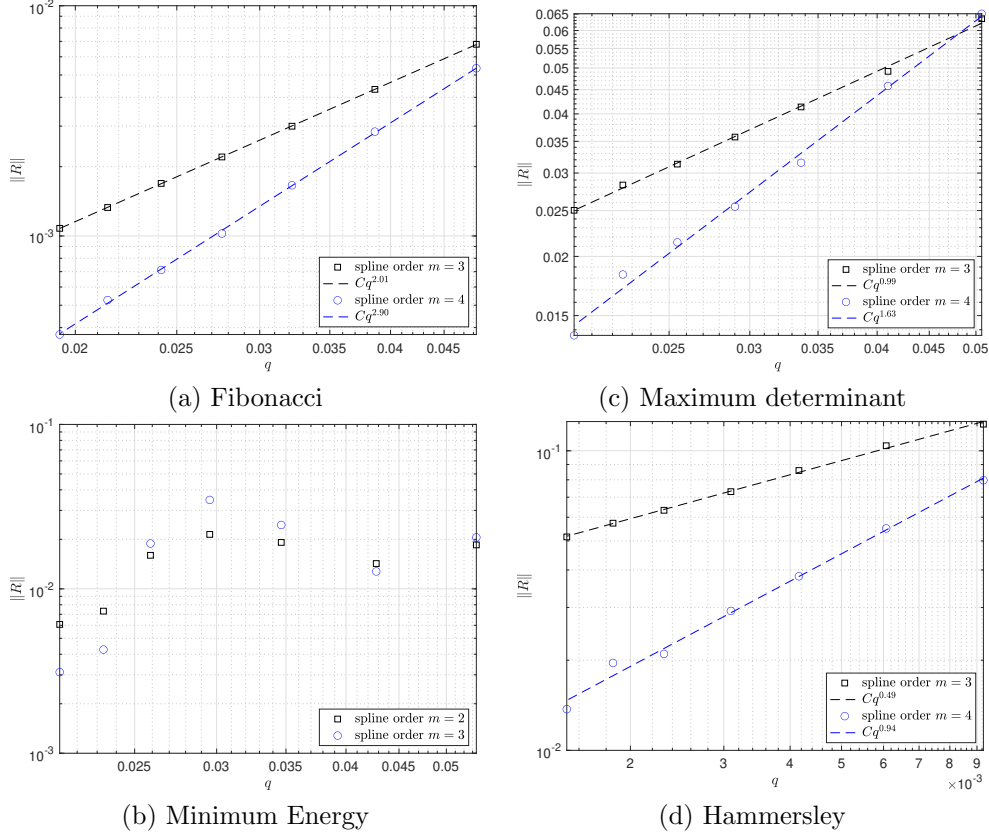


Figure 3: Numerical results on $\|\mathbf{R}\|$ vs. the separation radius q for different point set families on \mathbb{S}^2 using $\mathcal{L} = -\Delta$. Each plot shows the results for the restricted surface (32) spline kernels of order $m = 3$ and $m = 4$ using augmented spherical harmonic spaces Π_{m-1} . The dashed lines in (a), (c), & (d) show the lines of best fit (on a log-scale) to the data, which indicate an algebraic decay rate of $\|\mathbf{R}\|$ with decreasing q . The results in (b) do not show a discernible pattern of $\|\mathbf{R}\|$ in terms of q , so the estimated rates are omitted.

4.5 Numerical estimates on $\|\mathbf{R}\|$

In this section, we give numerical evidence that much better estimates for $\|\mathbf{R}\|$ than (31) may be possible. We consider DMs for $\mathcal{L} = -\Delta$ on \mathbb{S}^2 using the four families of point sets discussed in section 2 and illustrated in Figure 2.

We first consider DMs formed from the restricted surface spline kernels:

$$\Phi_m(x, y) = C_m(1 - x \cdot y)^{m-1} \log(1 - x \cdot y). \quad (32)$$

These kernels are CPD of order \tilde{m} , where $\tilde{m} \geq m$, and have a Mercer-like expansion (6) with coefficients that decay like $c_\ell \sim |\nu_\ell|^{-m}$ for $\ell \geq m$. Indeed, for $\ell \geq m$, the kernel has expansion (6) with coefficients satisfying $c_\ell = C \prod_{j=0}^{m-1} (\nu_\ell + j(j+1))^{-1}$ by [25, Lemma 3.4]. We consider the $m = 3$ and $m = 4$ kernels with augmented spherical harmonic spaces Π_{m-1} (the minimum degree space required for well-posedness). Figure 3 displays the results of $\|\mathbf{R}\|$ computed for points X of increasing cardinality N (and hence decreasing q) from each family of point sets. Included in the plots from (a), (c), & (d) of this figure are the estimated algebraic rates of decay of $\|\mathbf{R}\|$ in terms of decreasing q ; these estimates were omitted from (b) since no discernible pattern was evident. We note that the estimated rates in the three figures all involve positive powers of q rather than negative powers as in the bound (31). Furthermore, even the results in (b) do not follow (31).

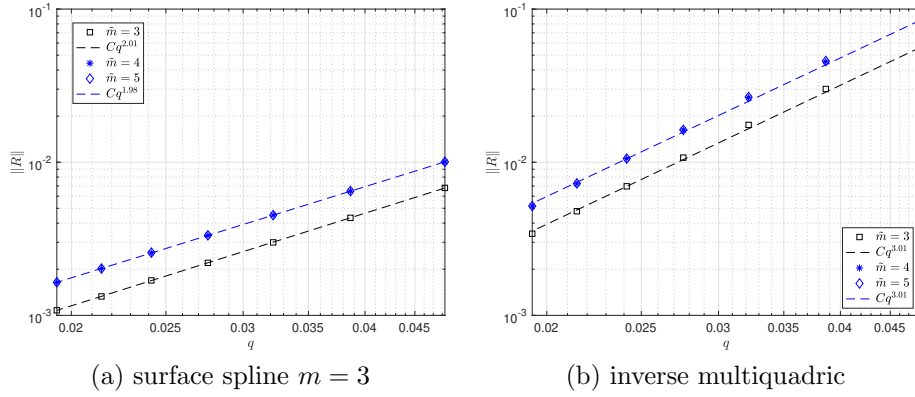


Figure 4: Numerical results on $\|\mathbf{R}\|$ vs. the separation radius q for the Fibonacci points on \mathbb{S}^2 using $\mathcal{L} = \Delta$. (a) Results from three experiments with the order of the restricted surface spline kernel (32) fixed at $m = 3$ and the degree of augmented spherical harmonic spaces $\Pi_{\tilde{m}-1}$ changing. (b) Same as (a), but for the restricted inverse multiquadric kernel. Dashed lines estimate the algebraic decay rate of $\|\mathbf{R}\|$ with decreasing q .

In the next experiment we test how $\|\mathbf{R}\|$ depends on the degree of the augmented spherical harmonic basis $\Pi_{\tilde{m}-1}$, $\tilde{m} \geq m$, when the kernel is fixed. This is especially common for applications of kernel-based methods on \mathbb{S}^2 (and more general domains) where the order of the spline kernel is kept low and the degree of the polynomial basis is allowed to grow [5, 37]. Figure 4 (a) shows the results for the Fibonacci nodes. We see from this plot that increasing the degree does not change the algebraic rate of decay of $\|\mathbf{R}\|$ with decreasing q , but only (possibly) the constant. We note that similar results were observed for the maximum determinant and Hammersley points and are thus omitted.

Finally, we consider the behavior of $\|\mathbf{R}\|$ for the restricted inverse multiquadric kernel $\Phi(x, y) = (1 + \varepsilon^2(1 - x \cdot y))^{-1/2}$, where $\varepsilon > 0$ is the free shape parameter. This kernel is PD with coefficients c_ℓ in (6) that decay exponentially fast with ℓ [4]. Hence, the estimates for bounding $\|\mathbf{R}\|$ in (31) do not apply. Figure 4 (b) displays the results associated with this kernel using the Fibonacci nodes. Similar to part (a) we include results for $\|\mathbf{R}\|$ when including different augmented spherical harmonic bases $\Pi_{\tilde{m}-1}$ with this kernel. As with the restricted surface spline results, $\|\mathbf{R}\|$ seems to have an algebraic decay rate (of approximately 3) with decreasing q and this rate does not seem to depend on \tilde{m} . We note that similar results were observed (with different algebraic rates) for the other point set families and hence are omitted.

These experiments suggest that the estimate in (31) is indeed overly pessimistic and better bounds for $\|\mathbf{R}\|$ may be possible, even ones that extend to kernels with exponentially decaying Mercer expansions. Unfortunately, the geometry of the points seems to affect the algebraic decay of $\|\mathbf{R}\|$ with decreasing q , so any tighter estimates may need to take the geometry into account.

5 Applications

In this section consider two applications of the theory of sections 3 and 4.

5.1 Continuous time-stability for the global DMs

Consider the semi-discrete approximation of the equation $\frac{\partial}{\partial t} u = \mathcal{L}u$ at a set of points $X \subset \mathbb{S}^d$, where $\mathcal{L} = p(\Delta)$ and $\sigma(\mathcal{L}) \subset (-\infty, 0]$ (e.g., for $\mathcal{L} = \Delta$ corresponding to the

diffusion equation). We denote the approximation as

$$\frac{d}{dt}u_X = \mathbf{M}_X u_X, \quad (33)$$

where $u_X : [0, \infty) \times X \mapsto \mathbb{R}$ and \mathbf{M}_X is the global DM associated with a PD or CPD kernel Φ .

A straightforward application of the results from sections 3 and 4 can be used to show the solution of the semi-discrete system is energy stable, and thus the norm of $u_X(t)$ does not grow in time. The proofs differ depending on the kernel Φ used to construct \mathbf{M}_X .

PD Kernel Using the norm $\|u\|_{\Phi_X^{-1}}^2 := u^T \Phi_X^{-1} u$, we note that

$$\frac{d}{dt} \|u_X\|_{\Phi_X^{-1}}^2 = u_X^T (\mathbf{M}_X^T \Phi_X^{-1} + \Phi_X^{-1} \mathbf{M}_X) u_X$$

which implies, using (7) that $\frac{1}{2} \frac{d}{dt} \|u_X\|_{\Phi_X^{-1}}^2 = u_X^T \Phi_X^{-1/2} \mathbf{K}_X \Phi_X^{-1/2} u_X < 0$, so the semi-discrete problem (33) is energy stable.

CPD Kernel In this case, we employ the semi-norm $[u]_{\mathbf{A}}^2 := u^T \mathbf{A} u$ where \mathbf{A} is the positive semi-definite matrix given in (11). Then

$$\frac{d}{dt} [u_X]_{\mathbf{A}}^2 = u_X^T (\mathbf{M}_X^T \mathbf{A} + \mathbf{A} \mathbf{M}_X) u_X$$

which implies, since $\mathbf{A} \mathbf{P} = 0$, that

$$\frac{1}{2} \frac{d}{dt} [u_X]_{\mathbf{A}}^2 = u_X^T \mathbf{A} \mathbf{K}_X \mathbf{A} u_X = (\mathbf{W}^T u_X)^T \widehat{\mathbf{A}} \widehat{\mathbf{K}}_X \widehat{\mathbf{A}} (\mathbf{W}^T u_X).$$

Here we have used (13) and the change of basis (16). Since $\widehat{\mathbf{K}}_X$ has negative spectrum, we have $\frac{d}{dt} [u_X]_{\mathbf{A}}^2 < 0$ as long as $\mathbf{W}^T u_X \neq 0$. However, if $\mathbf{W}^T u_X = 0$, then $u_X \in \Pi_{\tilde{m}-1}(X)$, in which case \mathbf{M}_X is exact and we can use the standard ℓ_2 norm to show $\frac{d}{dt} \|u_X\|^2 \leq 0$. Thus, the semi-discrete problem (33) is energy stable also for the CPD case.

5.2 Spectral stability of the local Lagrange DMs from restricted surface splines

We apply the results of section 4 to the restricted surface spline kernels Φ_m on \mathbb{S}^2 defined in (32). Recall that Φ_m is CPD of order \tilde{m} as long as $\tilde{m} \geq m$.

When $\tilde{m} = m$, these kernels have the property, introduced in [17], that for quasi-uniform point sets X , the kernel spaces $S_X(\Phi_m)$ possess a *localized basis*: a basis $(b_j)_{j \leq N}$, which enjoys the following two properties (among others)

- each function b_j employs a small stencil: $b_j \in S_{\Upsilon_j}(\Phi)$ where $\Upsilon_j \subset X$ consists of points near to x_j ,
- each b_j is close to χ_j in a variety of norms (roughly, for the norm of any Banach space in which the native space is embedded – this will be made more precise below).

The sphere, along with Euclidean space, provides the most readily available kernels having localized bases, although they exist in other settings as well. For any general compact, closed Riemannian manifold, there exist PD kernels with this property, as shown in [26], although they generally do not have convenient closed form expressions, or even expansions of the form (6) in a familiar orthonormal set. For compact, rank 1 symmetric spaces (which include spheres of all dimensions, as well as a number of other sphere-like manifolds), there exist kernels with Mercer-like expansions in the Laplacian eigenbasis, as shown in [24], for which the ideas of [17] can be applied to construct localized bases – in particular, this is possible for restricted surface splines and similar kernels on higher dimensional spheres.

Perturbation of the DM via localized bases Let $X \subset \mathbb{S}^2$ have mesh ratio $\rho := h/q$. For $K > 0$, and for $x_j \in X$, we define the stencil $\Upsilon_j := X \cap B(x_j, Kh|\log h|) \subset X$, and note that Υ_j has cardinality $\#\Upsilon_j \sim K^2\rho^2(\log h)^2 = \mathcal{O}(K^2(\log N)^2)$.

We define the local Lagrange function $b_j \in S_{\Upsilon_j}(\Phi_m)$ via the condition

$$b_j(x_k) = \delta_{j,k}, \quad \text{for all } x_k \in \Upsilon_j.$$

Note that $b_j \in S_X(\Phi_m)$, since $\Upsilon_j \subset X$. By [12, Lemma 5.2], there exist positive constants α and β so that for any stencil parameter $K > 0$ and for sufficiently dense $X \subset \mathbb{S}^2$,

$$\|\mathcal{L}b_j - \mathcal{L}\chi_j\|_{L_\infty(\mathbb{S}^2)} \leq Ch^J \quad \text{holds with } J = \alpha K + \beta.$$

The local Lagrange DM, \mathbf{M}_X^{LL} , is constructed by applying \mathcal{L} to each b_j :

$$\left(\mathbf{M}_X^{\text{LL}}\right)_{j,k} = \begin{cases} \mathcal{L}b_k(x_j), & |x_j - x_k| \leq Kh|\log h|, \\ 0, & \text{otherwise.} \end{cases}$$

Since X has mesh-ratio ρ the stencil Υ_j has cardinality $\#\Upsilon_j \leq C\rho^2(K^2(\log N)^2)$. Thus there are $\mathcal{O}(K^2(\log N)^2)$ nonzero entries in each row (or column) of \mathbf{M}_X^{LL} . Following the arguments in [12], specifically estimates [12, (6.3)] and [12, (5.9)], we have that

$$\|\mathbf{M}_X - \mathbf{M}_X^{\text{LL}}\|_2 \leq Ch^{J-2}. \quad (34)$$

We note that the approximation *order* J given by (34) has a linear dependence on the stencil parameter K , namely $J = \bar{\alpha}K + \bar{\beta}$ for some $\bar{\alpha}, \bar{\beta} \in \mathbb{R}$, with $\bar{\alpha} > 0$.

We can measure the distance between spectra of \mathbf{M}_X and \mathbf{M}_X^{LL} by using either Proposition 4.3 in the most general setting, or Theorem 4.5 in cases where \mathcal{L} separates Π_{m-1} from its orthogonal complement.

General (non-diagonalized) case We apply Proposition 4.3, with $\mathbf{M}^\epsilon = \mathbf{M}_X^{\text{LL}}$, and observe that for every eigenvalue $\mu \in \sigma(\mathbf{M}_X^{\text{LL}})$ there is $\mu^* \in \sigma(\mathbf{M}_X)$ for which $|\mu - \mu^*| \leq C\sqrt{\kappa\|\mathbf{R}\|}h^{J/2-1}$. At this point, we use the estimates on $\|\mathbf{V}\|$, $\|\mathbf{V}^{-1}\|$ and $\|\mathbf{R}\|$ collected in Corollary 4.6 to note that

$$\max_{\mu \in \sigma(\mathbf{M}_X^{\text{LL}})} \text{dist}(\mu, \sigma(\mathbf{M}_X)) \leq Ch^{J/2-1-3m/2}.$$

This suggests that J (and therefore K) should be chosen larger than $2m + 2$ in order to ensure fidelity to the original (positive) spectrum of \mathbf{M}_X .

Remark 5.1. *If the pessimistic bound $\|\mathbf{R}\| \leq Ch^{-3m}$ is replaced by $\|\mathbf{R}\| \leq C$, as suggested by the experimental results of section 4.5, then Corollary 4.6 gives the improved estimate*

$$\max_{\mu \in \sigma(\mathbf{M}_X^{\text{LL}})} \text{dist}(\mu, \sigma(\mathbf{M}_X)) \leq Ch^{J/2-1-m/2}.$$

Diagonalizable case If \mathcal{L} satisfies $\gamma = \min_{\ell \geq \tilde{m}} p(\nu_\ell) - \max_{\ell < \tilde{m}} p(\nu_\ell) > 0$, then we may apply Theorem 4.5 to obtain

$$\max_{\mu \in \sigma(\mathbf{M}_X^{\text{LL}})} \text{dist}(\mu, \sigma(\mathbf{M}_X)) \leq Ch^{J-2-5m}.$$

In particular, this holds if $\mathcal{L} = -\Delta$. (We recall that in this section we require $\tilde{m} = m$.)

Remark 5.2. *Here, as in Remark 5.1, if $\|\mathbf{R}\| \leq Ch^{-3m}$ is replaced by $\|\mathbf{R}\| \leq C$, as suggested by the experimental results of section 4.5, then Theorem 4.5 gives the improved estimate*

$$\max_{\mu \in \sigma(\mathbf{M}_X^{\text{LL}})} \text{dist}(\mu, \sigma(\mathbf{M}_X)) \leq Ch^{J-2-m}.$$

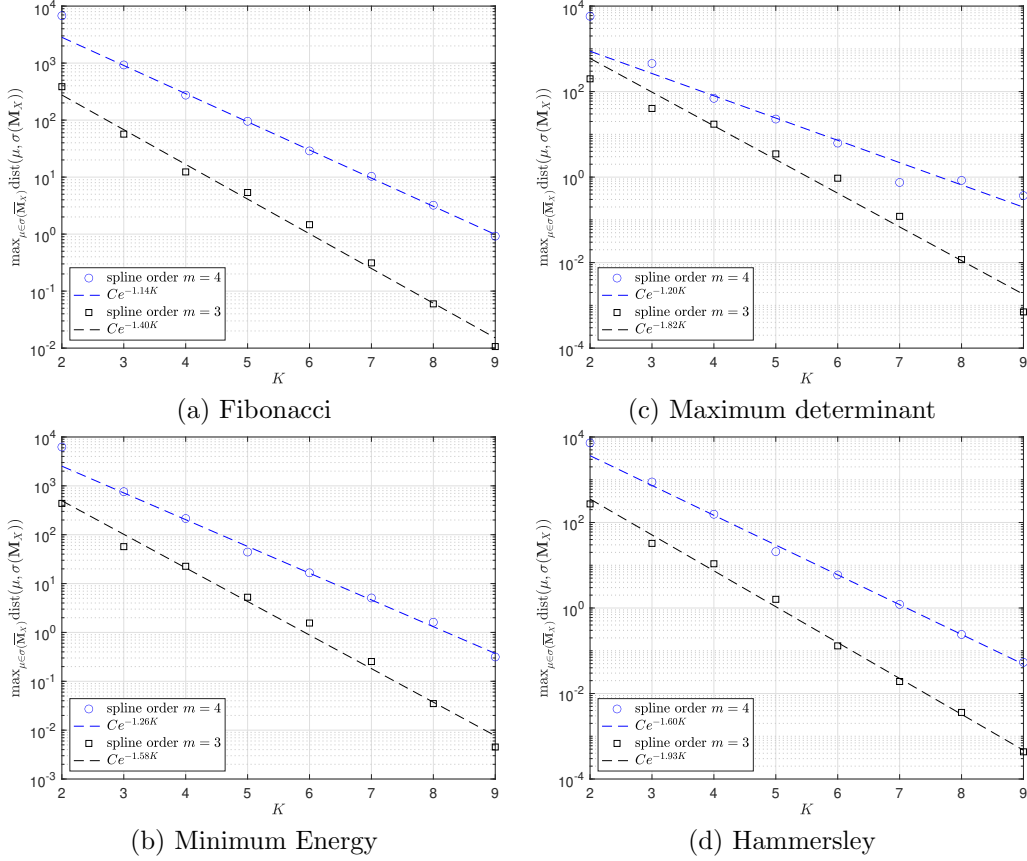


Figure 5: Numerical results comparing the maximum of the minimum distances between the spectra of the global DM (\mathbf{M}_X) and local Lagrange DM (\mathbf{M}_X^{LL}) as a function of the parameter K controlling the stencil size of the local Lagrange basis. Results are for $\mathcal{L} = \Delta$ computed from the restricted surface splines (32) of order $m = 3$ and $m = 4$ with augmented spherical harmonic spaces Π_{m-1} . Dashed lines are the lines of best fit (on a log-linear scale) to the data for $3 \leq K \leq 9$, which indicate an exponential decay rate with increasing K .

5.2.1 Numerical results on spectra of the local Lagrange DMs

The results from the previous section show that

$$\max_{\mu \in \sigma(\mathbf{M}_X^{LL})} \text{dist}(\mu, \sigma(\mathbf{M}_X)) = \max_{\mu \in \sigma(\mathbf{M}_X^{LL})} \min_{\mu^* \in \sigma(\mathbf{M}_X)} |\mu - \mu^*| \quad (35)$$

can be controlled by an expression of the form $h^{\alpha K + \beta}$ where $\alpha > 0$, although the precise dependence of α and β on m and \mathcal{L} are not easily determined analytically. In this section, we numerically examine the exponential decay of these bounds in terms of K for $\mathcal{L} = -\Delta$. Rather than choosing the support points in each stencil from a ball search with a radius that depends on K , we use a nearest neighbor search so that the cardinality of each stencil is fixed at

$$n = \lceil \frac{1}{7} K^2 (\log N)^2 \rceil. \quad (36)$$

For a quasi-uniform point set X , this gives similar results to a ball search. Additionally, this nearest neighbor approach with a fixed stencil size is more common in RBF-FD methods [14].

We again use the four families of point sets described in section 2 (and displayed in Figure 2): Fibonacci, minimum energy, maximum determinant, and Hammersley. As discussed in

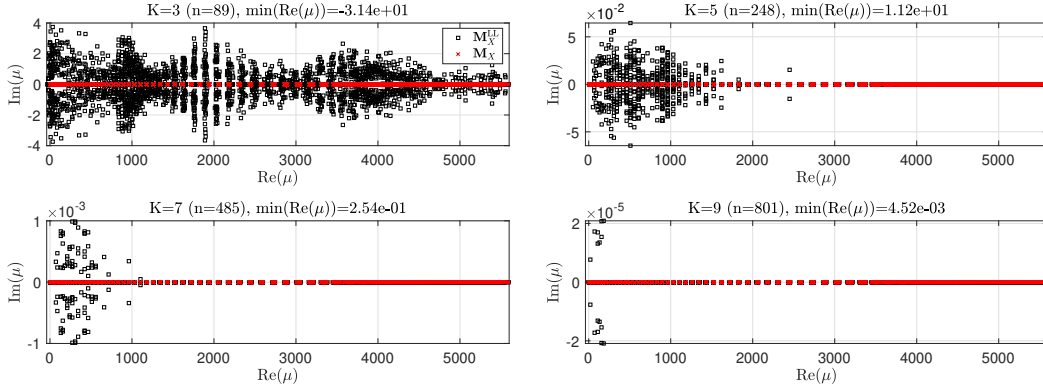


Figure 6: Comparison of the spectra of the global (\mathbf{M}_X) and local Lagrange (\mathbf{M}_X^{LL}) DMs based on different stencil sizes. Results are for the $\mathcal{L} = \Delta$ with $N = 4096$ minimum energy points and the kernel is the restricted surface spline kernel of order $m = 3$. The minimum real part of spectrum of \mathbf{M}_X^{LL} is listed in the title of each plot. Note the different scales for the vertical (imaginary) axes on each plot.

that section, the first three of these are quasi-uniform so the theory from the previous section applies. We also include results on the Hammersley points to see if this theory can potentially be generalized to more general point sets. For the numerical experiments we set $N = 4096$ for all but the Fibonacci nodes, where $N = 4097$ since they are only defined for odd numbers.

Figure 5 displays the results from the experiments for the restricted surface spline kernels of orders $m = 3$ and $m = 4$. We see from the figure that distance between the spectra (35) decreases exponentially fast with K for all four families of point sets, but that the rate depends on the geometry of the point set. We also see that the decay rate depends on the order m of the kernels as the estimates from the previous section predict.

To better compare the spectra of \mathbf{M}_X and \mathbf{M}_X^{LL} , we plot the entire spectrum of each matrix for the minimum energy points and four different K values in Figure 6. We see from the plots in this figure that as K increases the spread of the eigenvalues of \mathbf{M}_X^{LL} in the complex plane decreases. Additionally, for this point set, the real part of the spectrum of \mathbf{M}_X^{LL} is non-negative for all but the $K = 3$ case (see in the titles of the plots of the spectra).

5.3 Numerical results on spectra of the RBF-FD DMs

The RBF-FD method is similar to the local Lagrange method in that it produces a sparse DM, \mathbf{M}_X^{FD} , for approximating \mathcal{L} at a set of points X using kernel interpolation over local stencils of points. However, unlike the local Lagrange case, estimates are not yet available for bounding $\|\mathbf{M}_X - \mathbf{M}_X^{\text{FD}}\|$ so that the results of Proposition 4.3 or Theorem 4.5 can be applied to the spectral stability of \mathbf{M}_X^{FD} . In this section we numerically compare the stability of \mathbf{M}_X^{FD} in terms of \mathbf{M}_X using (36) to give evidence that similar bounds to the ones from Section 5.2 for \mathbf{M}_X^{LL} hold.

First, we briefly review the RBF-FD method for the case of surface splines on \mathbb{S}^2 ; see [14] for more general settings and details. Let $\Upsilon_j \subset X$ again denote a local stencil of points for each $x_j \in X$, and $u : \mathbb{S}^2 \rightarrow \mathbb{R}$ be some generic function. To approximate the operator $\mathcal{L}u$ at x_j , the RBF-FD method uses

$$\mathcal{L}u(x_j) \approx \sum_{k \in \sigma_j} \mathcal{L}\chi_k^{(j)}(x_j)u(x_k),$$

where $\chi_k^{(j)}$ are *stencil Lagrange functions* associated with Υ_j and σ_j is the index set for the stencil Υ_j in the global node set X . The stencil Lagrange functions are in the space S_{Υ_j}

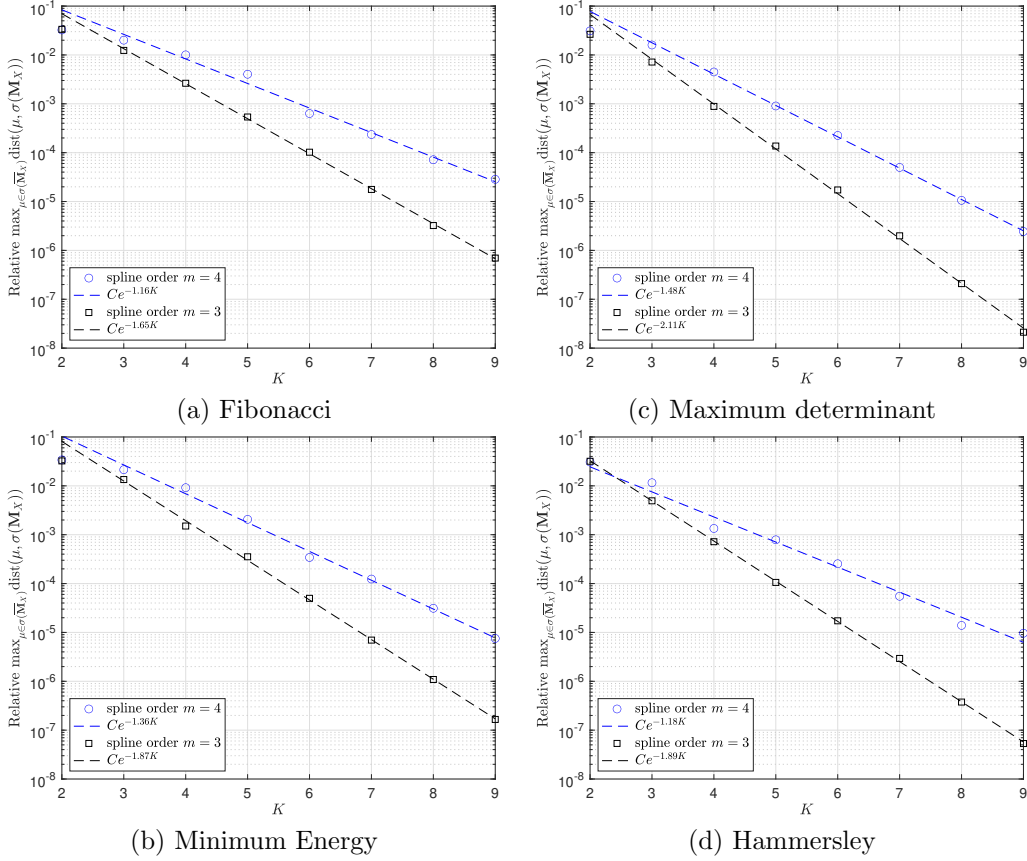


Figure 7: Same as Figure 5, but for the RBF-FD DM (\mathbf{M}_X^{FD}).

defined in (5) and satisfy $\chi_k^{(j)}(x_i) = \delta_{i,k}$ for $i, k \in \sigma_j$. The entries of RBF-FD DM are then given as follows:

$$\left(\mathbf{M}_X^{\text{FD}}\right)_{j,k} = \begin{cases} \mathcal{L}\chi_k^{(j)}(x_j), & k \in \sigma_j \\ 0, & \text{otherwise.} \end{cases}$$

The difference between the local Lagrange and RBF-FD methods may be subtle, but it is important. The latter is based on a separate interpolant over the stencil Υ_j defined by the target point x_j , while the former is based on interpolants defined over all stencils that have a non-empty intersection with the target point x_j . The RBF-FD method is then necessarily exact on the space $\Pi_m(X)$, but the local Lagrange method is not. We finally note that both methods produce \mathbf{M}_X in the limit that each stencil includes every point in X , i.e., $\Upsilon_j = X$.

For the numerical results, we follow exactly the same set-up as the previous section and compare the spectra of \mathbf{M}_X^{FD} to \mathbf{M}_X using the measure (35) for different K and surface spline orders m . We note that since \mathbf{M}_X^{FD} is exact on $\Pi_m(X)$ its spectrum will included $\Lambda_{m-1} = \{\lambda_\ell\}_{\ell=0}^{m-1}$, where are the first $m-1$ eigenvalues of \mathcal{L} .

Figure 7 displays the results from the experiments. Similar to the local Lagrange case, we see from the figure that the distance between the spectra (35) for \mathbf{M}_X^{FD} also decreases exponentially fast with K for all four families of point sets. This indicates that similar bounds to those from Section 5.2 for \mathbf{M}_X^{LL} may also hold for \mathbf{M}_X^{FD} .

The spectra of \mathbf{M}_X and \mathbf{M}_X^{FD} are directly compared in Figure 8 for the minimum energy points. We see from this figure that for the same K the spectrum of \mathbf{M}_X^{FD} does not extend as far in the complex plane as the spectrum of \mathbf{M}_X^{LL} given in Figure 6. Additionally, the rate at which the spectrum approaches the positive real axis as K increases is higher for the

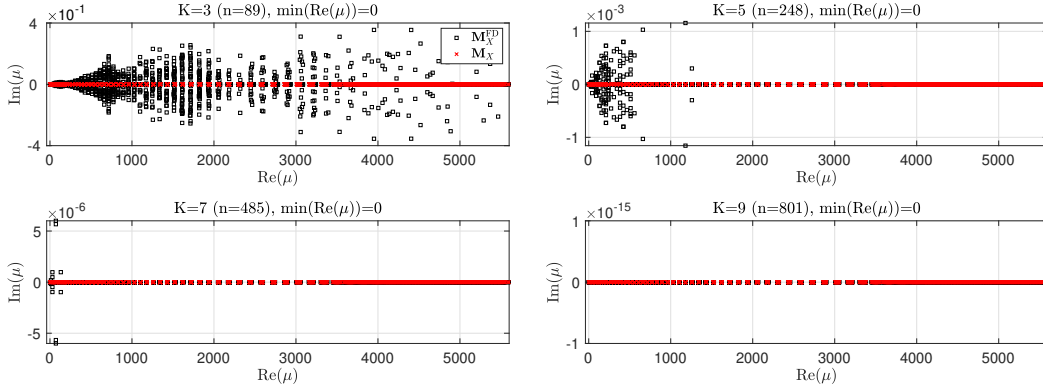


Figure 8: Same as Figure 6, but for the RBF-FD DM (\mathbf{M}_X^{FD}).

RBF-FD method. Finally, the figure shows that for each K the eigenvalue of \mathbf{M}_X^{FD} with the smallest real part is 0, which is the expected value for $\mathcal{L} = -\Delta$.

6 Concluding remarks

The results of this paper have addressed important issues regarding the spectrum of DMs that arise in global and local kernel collocation methods and their stability under perturbations. However, there remain significant open questions in both the global and the local cases. We briefly note three interesting open problems:

- There is more to temporal stability of method of lines (or semi-discrete) approximations like (33) considered in section 5.1 than the spectrum of the DM \mathbf{M}_X or the energy stability of the solutions of (33). Showing stability for the fully discrete problem (i.e., after discretizing (33) in time) requires addressing questions about the pseudospectra (resolvent stability) [42] or strong stability [30] of the DMs. In the latter case, [30, Section 3.1] considers the coercivity condition

$$\Re\langle u, \mathbf{M}_X u \rangle_* \leq -\eta \|\mathbf{M}_X u\|_*^2, \quad \eta > 0,$$

of a matrix in some inner product $\langle \cdot, \cdot \rangle_*$ (this is [30, (3.2)]). Coercivity guarantees stability of certain Runge-Kutta method applied to (33) provided a CFL-type condition holds.

- If $\sigma(\mathcal{L}) \subset (-\infty, 0]$ and $0 \in \sigma(\mathcal{L})$, then a perturbed DM \mathbf{M}^ϵ may fail to inherit the Hurwitz stability of \mathbf{M}_X . In short, the results presented here do not guarantee that perturbation preserves weak Hurwitz stability (semi-stability).
- The challenge of obtaining useful perturbation errors for \mathbf{M}_X^{FD} that are similar to (34) amounts to controlling the difference $\mathcal{L}\chi_k^{(j)}(x_j) - \mathcal{L}\chi_j(x_j)$. Superficially, this may seem similar to $\mathcal{L}b_j(x_j) - \mathcal{L}\chi_j(x_j)$, but the challenge stems from the fact that the center x_k associated with $\chi_k^{(j)}$ may be situated near to the boundary of the domain of $B(x_j, Kh|\log h|)$, which is where the decay conditions of the Lagrange functions are not yet well understood.

References

- [1] Milton Abramowitz and Irene A Stegun. *Handbook of mathematical functions with formulas, graphs, and mathematical tables*, volume 55. National bureau of standards, 1964.

- [2] Richard H. Bartels and George W Stewart. Solution of the matrix equation $AX + XB = C$ [f4]. *Communications of the ACM*, 15(9):820–826, 1972.
- [3] Friedrich L Bauer and Charles T Fike. Norms and exclusion theorems. *Numerische Mathematik*, 2:137–141, 1960.
- [4] Brad JC Baxter and Simon Hubbert. Radial basis functions for the sphere. In *Recent Progress in Multivariate Approximation: 4th International Conference, Witten-Bommerholz (Germany), September 2000*, pages 33–47. Springer, 2001.
- [5] Victor Bayona, Natasha Flyer, Bengt Fornberg, and Gregory A Barnett. On the role of polynomials in RBF-FD approximations: II. Numerical solution of elliptic PDEs. *J. Comput. Phys.*, 332:257–273, 2017.
- [6] Michele Benzi, Gene H Golub, and Jörg Liesen. Numerical solution of saddle point problems. *Acta numerica*, 14:1–137, 2005.
- [7] William Gee Bickley and J McNamee. Matrix and other direct methods for the solution of systems of linear difference equations. *Philosophical Transactions of the Royal Society of London. Series A, Mathematical and Physical Sciences*, 252(1005):69–131, 1960.
- [8] Debao Chen, Valdir Menegatto, and Xingping Sun. A necessary and sufficient condition for strictly positive definite functions on spheres. *Proceedings of the American Mathematical Society*, 131(9):2733–2740, 2003.
- [9] King-wah Eric Chu. Generalization of the Bauer-Fike theorem. *Numerische Mathematik*, 49:685–691, 1986.
- [10] Oleg Davydov. Error bounds for a least squares meshless finite difference method on closed manifolds. *Advances in Computational Mathematics*, 49(4):48, 2023.
- [11] Harold Donnelly. Bounds for eigenfunctions of the Laplacian on compact Riemannian manifolds. *Journal of Functional Analysis*, 187(1):247–261, 2001.
- [12] Wolfgang Erb, Thomas Hangelbroek, Francis J. Narcowich, Christian Rieger, and Joseph D. Ward. Highly localized RBF Lagrange functions for finite difference methods on spheres, 2023.
- [13] Natasha Flyer and Grady B Wright. A radial basis function method for the shallow water equations on a sphere. In *Proceedings of the Royal Society of London A: Mathematical, Physical and Engineering Sciences*, pages rsaa–2009. The Royal Society, 2009.
- [14] B. Fornberg and N. Flyer. Solving PDEs with radial basis functions. *Acta Numer.*, 24:215–258, 2015.
- [15] B. Fornberg and E. Lehto. Stabilization of RBF-generated finite difference methods for convective PDEs. *Journal of Computational Physics*, 230:2270–2285, 2011.
- [16] Bengt Fornberg and Natasha Flyer. *A Primer on Radial Basis Functions with Applications to the Geosciences*. Society for Industrial and Applied Mathematics, Philadelphia, PA, USA, 2015.
- [17] E. Fuselier, T. Hangelbroek, F. J. Narcowich, J. D. Ward, and G. B. Wright. Localized bases for kernel spaces on the unit sphere. *SIAM J. Numer. Anal.*, 51(5):2538–2562, 2013.
- [18] Edward Fuselier and Grady B Wright. Scattered data interpolation on embedded sub-manifolds with restricted positive definite kernels: Sobolev error estimates. *SIAM Journal on Numerical Analysis*, 50(3):1753–1776, 2012.

- [19] Edward J Fuselier and Grady B Wright. A high-order kernel method for diffusion and reaction-diffusion equations on surfaces. *Journal of Scientific Computing*, 56(3):535–565, 2013.
- [20] Q. T. Lê Gia. Approximation of parabolic PDEs on spheres using spherical basis functions. *Adv. Comput. Math.*, 22:377–397, 2005.
- [21] Jan Glaubitz, Jan Nordström, and Philipp Öffner. Summation-by-parts operators for general function spaces. *SIAM Journal on Numerical Analysis*, 61(2):733–754, 2023.
- [22] John B Greer, Andrea L Bertozzi, and Guillermo Sapiro. Fourth order partial differential equations on general geometries. *Journal of Computational Physics*, 216(1):216–246, 2006.
- [23] Michael Griebel, Christian Rieger, and Barbara Zwicknagl. Regularized kernel-based reconstruction in generalized besov spaces. *Foundations of Computational Mathematics*, 18:459–508, 2018.
- [24] T. Hangelbroek, F. J. Narcowich, and J. D. Ward. Polyharmonic and related kernels on manifolds: interpolation and approximation. *Found. Comput. Math.*, 12(5):625–670, 2012.
- [25] Thomas Hangelbroek. Polyharmonic approximation on the sphere. *Constructive Approximation*, 33(1):77–92, 2011.
- [26] Thomas Hangelbroek, Francis J Narcowich, Christian Rieger, and Joseph D Ward. Direct and inverse results on bounded domains for meshless methods via localized bases on manifolds. *Contemporary Computational Mathematics-A Celebration of the 80th Birthday of Ian Sloan*, pages 517–543, 2018.
- [27] D. P. Hardin, T. Michaels, and E. B. Saff. A comparison of popular point configurations on S^2 . *Dolomites Res. Notes Approx.*, 9:16–49, 2016.
- [28] Nick Higham. What is the Sylvester equation? <https://nhigham.com/2020/09/01/what-is-the-sylvester-equation/>.
- [29] E Lehto, V Shankar, and G. B. Wright. A radial basis function (RBF) compact finite difference (FD) scheme for reaction-diffusion equations on surfaces. *SIAM J. Sci. Comput.*, 39:A219–A2151, 2017.
- [30] Doron Levy and Eitan Tadmor. From semidiscrete to fully discrete: Stability of Runge–Kutta schemes by the energy method. *SIAM review*, 40(1):40–73, 1998.
- [31] Valdir Antônio Menegatto and Ana Paula Peron. Conditionally positive definite kernels on euclidean domains. *Journal of mathematical analysis and applications*, 294(1):345–359, 2004.
- [32] Claus Müller. *Spherical harmonics*, volume 17. Springer, 2006.
- [33] Francis J Narcowich, Pencho Petrushev, and Joseph D Ward. Localized tight frames on spheres. *SIAM Journal on Mathematical Analysis*, 38(2):574–594, 2006.
- [34] Dang Thi Oanh, Oleg Davydov, and Hoang Xuan Phu. Adaptive rbf-fd method for elliptic problems with point singularities in 2d. *Applied Mathematics and Computation*, 313:474 – 497, 2017.
- [35] Rodrigo B Platte and Tobin A Driscoll. Eigenvalue stability of radial basis function discretizations for time-dependent problems. *Computers & Mathematics with Applications*, 51(8):1251–1268, 2006.

- [36] Gabriele Santin and Robert Schaback. Approximation of eigenfunctions in kernel-based spaces. *Advances in Computational Mathematics*, 42:973–993, 2016.
- [37] Varun Shankar and Aaron L. Fogelson. Hyperviscosity-based stabilization for radial basis function-finite difference (RBF-FD) discretizations of advection-diffusion equations. *J. Comput. Phys.*, 372:616–639, 2018.
- [38] Varun Shankar, Grady B. Wright, Robert M. Kirby, and Aaron L. Fogelson. A radial basis function (RBF)-finite difference (FD) method for diffusion and reaction-diffusion equations on surfaces. *J. Sci. Comput.*, 63(3):745–768, 2014.
- [39] Christopher D Sogge. Concerning the L^p norm of spectral clusters for second-order elliptic operators on compact manifolds. *Journal of Functional Analysis*, 77(1):123–138, 1988.
- [40] Igor Tominec, Elisabeth Larsson, and Alfa Heryudono. A least squares radial basis function finite difference method with improved stability properties. *SIAM Journal on Scientific Computing*, 43(2):A1441–A1471, 2021.
- [41] Igor Tominec, Murtazo Nazarov, and Elisabeth Larsson. Stability estimates for radial basis function methods applied to time-dependent hyperbolic pdes. *arXiv preprint arXiv:2110.14548*, 2021.
- [42] Lloyd N. Trefethen and Mark Embree. *Spectra and Pseudospectra: The Behavior of Nonnormal Matrices and Operators*. Princeton University Press, Princeton, 2005.
- [43] Holger Wendland. *Scattered data approximation*, volume 17. Cambridge university press, 2004.
- [44] Holger Wendland and Jens Künemund. Solving partial differential equations on (evolving) surfaces with radial basis functions. *Advances in Computational Mathematics*, 46:64, 2020.